International Journal of Computer Science in Sport

Volume 6/Edition 1

ISSN 1684-4769

TABLE OF CONTENTS

Editorial

Arnold Baca

Department of Biomechanics, Kinesiology and Applied Computer Science,

ISW, University of Vienna

Dear readers:

One month has passed since the very successful 6th International Symposium on **Computer Science in Sport** organized by Larry Katz and Ruth Morey-Sorrentino at the University of Calgary, 3-6 June 2007. Delegates from 23 nations participated in this event. Excellent presentations were given during this conference. Selected authors will be invited to submit their papers for publication within this journal.

Five original papers have been included within this issue.

E. Pogalin, **A.H.C. Thean**, **J. Baan**, **N.W. Schipper** and **A.W.M. Smeulders** discuss the application of video analysis for training registration in swimming. Results from a prototype system are described.

In the paper by **F. Leboeuf, G. Bessonnet** and **P. Lacouture** a parametric optimization technique is applied to simulate the flight phase of somersaults. The gymnast is modelled as a planar seven-segment multibody system with six internal degrees of freedom. Simulation results show real similarities with human somersaults.

L. Valandro, **L. Colombo**, **H. Cao**, **F. Recknagel**, **S. Dun** and **E.L. Secco** investigate the relationship between ball speed and anthropometrical characteristics of professional baseball pitchers using an evolutionary algorithm. The authors assume that their findings could have some relevance for bio-inspired robotics.

The report "sail:lab" by **F. Bünger**, **S. Busch**, **I. Gasser**, **S. Günzel**, **A. Hebbel-Seeger** and **M. Mohr** describes an interdisciplinary project of mathematicians and sport scientists. E-Learing components for sailing simulation have been developed, which can be integrated in Blended Learning scenarios for students of both disciplines.

Attitudes and behaviours of Greek Pysical Education students towards the use of computers are investigated in the project report **by E. Bebetsos**, **O. Kouli** and **P. Antoniou**

If you have any questions, comments, suggestions and points of criticism, please send them to me.
Enjoy the summer!

Arnold Baca, Editor in Chief
University of Vienna, arnold.baca@iacss.org

Video-based Training Registration for Swimmers

E. Pogalin[1,2], A.H.C. Thean[2], J. Baan[2], N.W. Schipper[2], A.W.M. Smeulders[1]

[1]Intelligent Systems Lab Amsterdam, Faculty of Science, University of Amsterdam, The Netherlands

[2]Business Unit Monitoring Systems, Netherlands Organization for Applied Scientific Research (TNO), The Netherlands

Abstract

During the last decade, performance improvements in top sports have been increasingly driven by technological innovations. This paper discusses the application of video analysis for training registration in swimming. In current practice, coaches have limited means to evaluate objectively and quantitatively how a training session was carried out. We propose the use of a video-based registration system in order to help the coach in acquiring such information. The system uses multiple cameras to cover the swimming pool. By using a simple background modeling and blob tracking method swimmers are tracked and their lap times are estimated. The main limitation of the system is the failure to detect swimmers at the pool ends while they are resting or underwater. This can lead to the necessity to perform manual interactions to associate laps to swimmers and a systematic underestimation of the lap times of typically 1.5 seconds. Our results can be used to formulate training guidelines that can help overcome some limitations of the system so that, with little or no manual effort, the system could be used in practice to do quantitative measurements. The information on the actual training performance of the swimmers could then be compared with the training schedule made beforehand and used to further optimize the training program.

KEY WORDS: TRAINING REGISTRATION, VIDEO ANALYSIS, TRACKING, SWIMMING

Introduction

In recent years, performance improvements on top sports have been more and more driven by technological innovations. The rapid development of computer and information technology creates new opportunities to analyze aspects of sports that were previously out of reach. One particular application of technology that is growing in popularity is the use of video to analyze sport training (Wang et al., 2004). For example, it has been used to analyze a hand-ball game (Perše et al., 2006), soccer (Xu et al., 2004) and golf (Urtasun et al., 2005). The goal of video analysis is to evaluate the athlete's performance during training sessions, thereby providing assistance to coaches and athletes. This paper will discuss the application of video analysis to swimming, in particular to the training sessions of top swimmers.
Using current practice, swimming coaches spend a lot of time making training programs, but they have few objective and quantitative measures to evaluate how the training was carried

out. The evaluation is limited to visual inspection and some time measurements with a stopwatch. At the end of the session, the swimmers fill in an evaluation form on how they experienced the session and to measure physical tiredness, lactate measurements are made by drawing blood samples. If several swimmers are training together the coach cannot give full attention to each of them and it is difficult to log all previous training data to make comparisons between training sessions. Our aim is to develop a video analysis system that will provide quantitative evaluation metrics for full training sessions of multiple swimmers and allow training schedules to be optimized.

In the last decade, video-based motion analysis has been used to improve technical performance in swimming. Usually underwater cameras are used to record swimmers and during playback the coach can show them where they should correct or improve the strokes. The interactive video software developed by Dartfish (Dartfish, 2006) has been used by many coaches all over the world. By inspecting the recording and manually inserting various markers on the video, the coach can measure aspects of the swimmer's motions. Another type of registration is hand force measurement, combined with video recording (STR, 2006). During the training, the developed Aquanex system measures the forces exerted by both hands in real-time. Analyzing the force curves in time makes it possible to reinforce the positive elements and identify the limiting factors. These systems are useful for giving detailed information about technique but not for registering the training sessions of multiple swimmers.

In terms of Computer Vision, the problem of monitoring swimmers is known as tracking persons in surveillance. In the last few years visual surveillance received growing attention (Hu et al., 2004). Two main approaches to this problem can be distinguished in literature, the motion-based approach and model-fitting approach.

The motion-based approach involves modeling the background scene and doing motion segmentation to detect foreground objects (see Stauffer & Grimson, 1999 and Elgammal et al., 2002). The background model is updated continuously to cope with scene variations and moving foreground objects are associated to previously-detected objects to form tracks. This approach has been applied to swimmers by Eng et al. (2006), who focused on drowning detection. Using this approach the object of interest is identified by its motion and this can have disadvantages when the tracked object stops moving. It is most appropriate for stationary cameras in scenes that do not show strong variation and is computationally efficient.

The model-fitting approach focuses on modeling the object to be tracked and fitting this model directly to the input data. Using this approach the object of interest is identified by its appearance and this can have disadvantages when the object appearance is highly-variable or unpredictable. Baumberg & Hogg (1995) and Gavrila & Philomin (1999) used a silhouette-based representation to track humans in video sequences, but when the object is partially occluded this method will not perform correctly. Nguyen & Smeulders (2004) learned the intensity pattern of the object of interest and the local surrounding background, which allowed robust tracking even under severe changes of both the foreground and the surrounding background. However, this algorithm has to be initialized manually and tracking multiple objects requires more computing power when compared to the first approach. Viola et al. (2005) introduced a method for detecting pedestrians in surveillance video which learns the appearance of full human figures from a large dataset. The trained pedestrian detector can be run in almost real-time (4 fps) but it does not perform well with partially-occluded human figures.

This paper presents results obtained with a prototype video analysis system based on a motion-based approach to swimmer tracking. The system is not required to work fully-automatically and is designed for compliant subjects who are willing to adhere to certain guidelines about behavior in a controlled environment. The results obtained allow us to identify important issues for the design of future systems. Our analysis includes considerations of hardware, swimming pool infrastructure, training schedule guidelines and interfaces but we pay particular attention to algorithm requirements and performance evaluation.

Methods

This section describes the hardware setup used to capture the training session, the data processing algorithm and the performance evaluation method used to analyze the results.

We recorded 45 minutes of video during training sessions of the Dutch youth national swimming team. Only three lanes were used during the training. The bottom lane was occupied by a single swimmer who swam back and forth in separate halves of the lane. The middle lane was occupied by two swimmers who each swam back and forth in separate halves of the lane. The third lane was occupied by four swimmers who swam in a circulating pattern i.e. swimmers moved in a different direction in each half of the lane. To have an overview of the whole 50m pool length we used 3 PAL cameras (with 720x576 pixels resolution each) with overlapping views elevated approximately 4m high at the pool side on tripods (Figure 1). The use of tripods is motivated by the fact that training sessions are often held in different pools so we need a mobile setup that can be easily built up and broken down. The cameras are connected to 3 frame grabbers that are installed on a dual-core Xeon 3GHz PC. Figure 2 shows the sample views from each camera.

Figure 1. The hardware setup used to record the training session. The 3 PAL cameras are elevated at the pool side on tripods.

Figure 2. Sample views from the three PAL cameras.

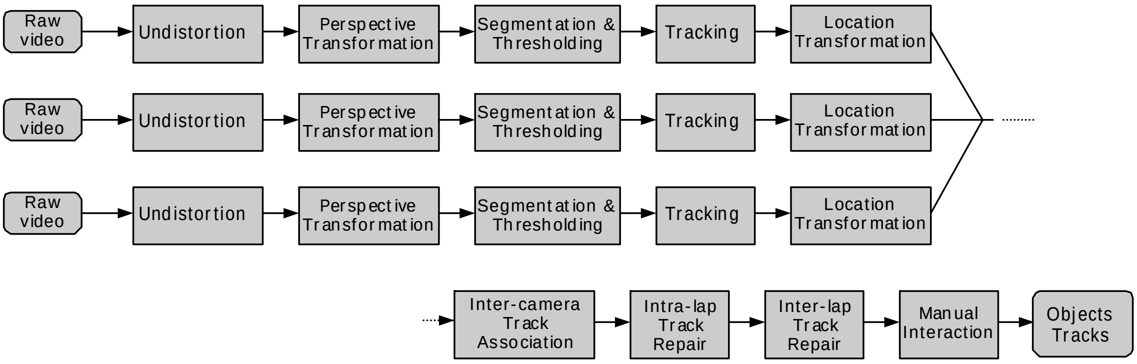

Figure 3. Block diagram of the data processing. The system uses the raw recording videos as input and produces object tracks as output.

The processing block diagram can be seen in Figure 3. The recordings made during data acquisition are the input of the processing. At the end, a list of objects tracks, which represent the swimmers laps, will be generated. The following list gives a short description of what each block does:

- *Undistortion:* This step corrects the distortion introduced by the lens. The distorted input image (Figure 2, left) is transformed to a rectified image (Figure 4, left). The camera distortion parameters are estimated beforehand using images of a calibration checkerboard in six orientations and the MATLAB Calibration Toolbox (Bouguet, 2006).

- *Perspective Transformation:* Perspective transformation is applied on sub-region of the image (e.g. yellow rectangle in Figure 4, left). This sub-region is defined manually for each camera and is specific to a given setup. The transform regularizes the geometry of the view and gives the impression of a view from directly above the pool (Figure 4, right).

- *Segmentation & Thresholding:* This step is used to separate the foreground from the background (See Figure for the detailed block diagram). Firstly, each RGB pixel of the input image is transformed to the red chrominance (Cr) component of the YCbCr color space using the following relation:

$$Cr = 128 - (0.4998R + 0.4185G + 0.08128B)$$

  Since the water has strong blue component and the swimmers have strong red component this transformation enhances the distance between the color of swimmers and the color of water. After this transformation, a background model B_t is built and updated continuously by taking the running average of image frames:

$$B_t = (1-\alpha)B_{t-1} + \alpha I_t$$

with I_t as the current frame and α the update rate (how fast the model forgets previous frames). Finally, the image difference between the current image and background model image is then transformed to binary image by using hysteresis thresholding (Davies, 2005) to obtain groups of pixels (blobs), which represents the swimmers. The low and high intensity thresholds were determined by visual inspection of the binary output image and set to 10 and 16 respectively. Only blobs containing more than 60 pixels are admitted to the output, because smaller blobs are likely to be the result of noise caused by water movements and so on.

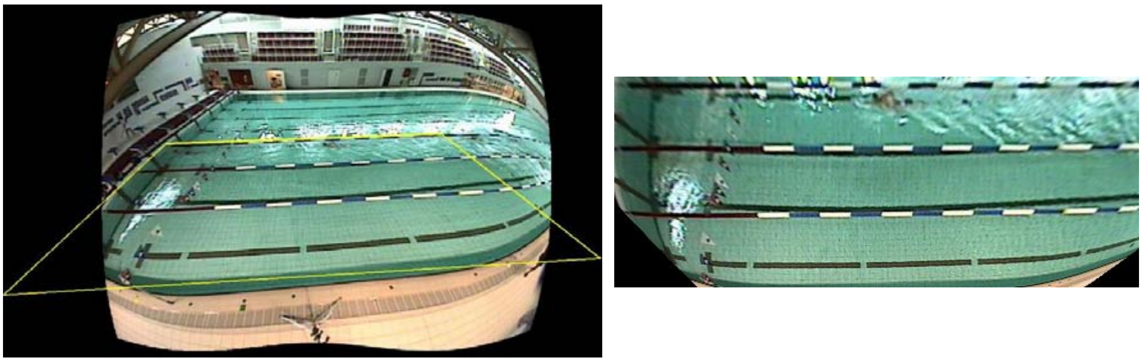

Figure 4. Perspective transformation from undistorted image. The region marked with the yellow rectangle on the left image is transformed to the right image. The rest of the image is discarded.

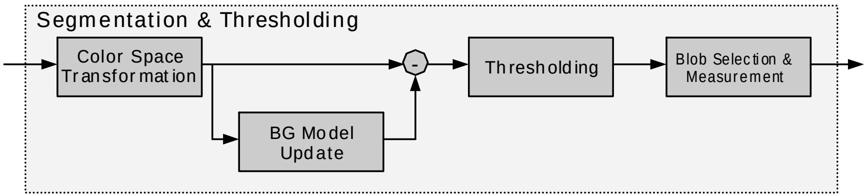

Figure 5. Detailed block diagram of the Segmentation & Tracking block.

- *Tracking*: This step associates blobs from previous video frames with the current one (Figure 6) to form tracks. If blobs from the current frame and the previous overlap they are associated. The interaction handling is used to deal with the cases when more than one association is possible. For example, when swimmers approach each other the segmentation step may detect a single blob containing multiple swimmers. This type of interaction is handled by considering the existing individual swimmer's tracks as lost (no association possible) and creating a new track for the combined blob. When the single blob splits again into two separate blobs, the track from the single blob is considered as lost and two new tracks are generated for each swimmer. If an existing track cannot be associated to a blob in the current frame (i.e. lost track), linear extrapolation of the blob motion is used to predict the blob position and associations to the predicted positions are possible for up to 10 frames, after which it will be removed from the active track list and passed on to the next processing step.

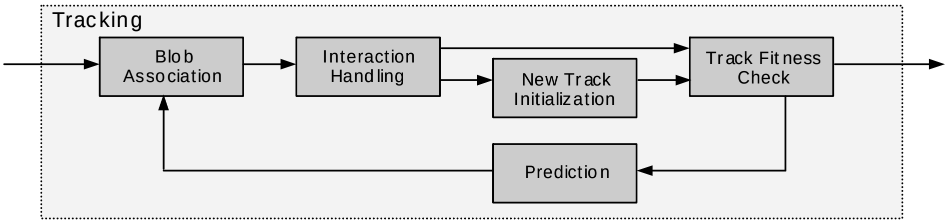

Figure 6. Detailed block diagram of the Tracking block.

- *Location Transformation:* This step performs a conversion from pixel coordinates to real world coordinates (i.e. meters). Since we know how long and how wide the pool is (the lane width is an official standard and the length can be determined by counting the stripes of the lane dividers), the pixel-to-world relationship can be calculated.
- *Inter-camera Track Association:* The track information from the multiple video streams is combined in this step. In the overlapping region between two camera views, tracks of swimmers leaving one view and entering an adjacent view are combined by associating tracks with the best degree of overlap. However, tracks observed to be traveling in opposite directions are not considered for association. This constraint is used because we know that swimmers should not turn back in the middle of the pool.
- *Intra-lap Track Repair:* Within a lap the track from a single swimmer may be fragmented (i.e. broken down into several short tracks). These track fragments can be grouped together using the following equations:

$$s_{i+1} = \arg\min_{s_j} d\left(\bar{s}'_{i,end}, \bar{s}_{j,start}\right), \quad \bar{s}_i = [x, y]^T, \ dir(s_i) = dir(s_j)$$

  where $d\left(\bar{s}_i, \bar{s}_j\right)$ is the Euclidean distance between two points, $\bar{s}_i$ the starting or end point of track s_i in 2D and $dir\left(s_i\right)$ is the motion direction of the specified track (either left or right). For each fragmented track s_i, the next track $s_{i+1} = s_j$ with the same direction of motion and minimum 2D Euclidean distance between the extrapolated end point of s_i' and the starting point of s_j is found. The end point of s_i is extrapolated to the candidate track starting point s_j in order to select the most probable candidate if there is a large gap between the current track and the next candidate track. Once a whole lap is recovered, the gaps between fragmented tracks are filled using linear interpolation.
- *Inter-lap Track Repair:* During the training session swimmers reaching the end of the pool either turn and start a new lap (usually performing a tumble turn), or take a rest. To maintain the track of a swimmer between laps the following rule is introduced. Any track that enters a region 5 meters from the end of the pool is associated to the next track that leaves that region as long as no other track enters the region in the meantime. When multiple tracks enter the region before any tracks leave it is not possible to maintain the track automatically (see Figure 7). These events are recognized automatically and require manual correction.

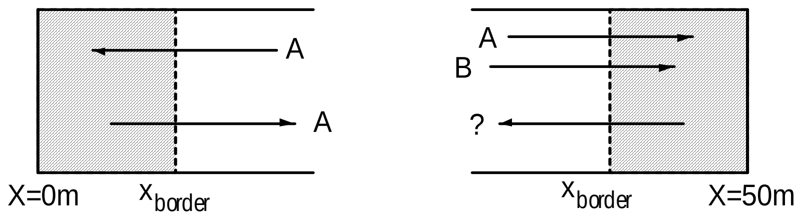

(a) (b)

Figure 7. The scheme used to group laps belonging to each swimmer in a lane, at the ends of the pool. (a) If one swimmer enters the region and some time later leaves and no other swimmers are resting, then the two laps can be easily grouped. (b) When multiple swimmers enter the region and some time later one swimmer leaves, two possibilities arise. Either swimmer A left first or swimmer B.

- *Manual Interaction:* The last step is to perform inter-lap track repair manually for those tracks that cannot be automatically associated. Since no user interface has yet been implemented this is done by inspecting the video and editing the results file.

Performance evaluation is done using two measures: frame-based metrics and object-based metrics (Bashir & Porikli, 2006). Firstly, a ground truth set is constructed and compared to the automatic detections in selected frames. Secondly, the individual tracks of objects are analyzed as separate entities. The ground truth set of swimmer locations was created using the ViPER tool (Doermann et al., 2000). We created a sparse set with an interval of 100 frames as a trade-off between amount of work needed and the reliability of the ground truth set. A bounding box covering the head and torso is used to represent the location of a swimmer. The arms and legs are excluded because they are underwater frequently, which make them difficult to use as a reliable boundary. Accurate lap times cannot be measured using a sparse ground truth so the start and end times for each lap were also noted: the start and end times are when the swimmers break or make contact with the pool wall, either by using their arms or feet.

Frame-based metrics measure how well the swimmers are detected in each frame. First, the following standard quantities were measured:

- True Positive (TP): The number of bounding boxes for which both ground truth data and system results agree on the presence of a swimmer.
- False Positive (FP): The number of bounding boxes for which the system falsely detects a swimmer.
- False Negative (FN)**:** The number of bounding boxes for which the system misses a swimmer.

In the above definitions, the matching between the ground truth data and the system results is done by looking at the overlap between the two. If the bounding box centre of the tracking results is located inside a ground truth bounding box, it is considered a match. Furthermore, the following metrics are derived from the above definitions:

- Tracker Detection Rate = TP / (FN + TP)
- False Alarm Rate = FP / (TP + FP)

These metrics were calculated for three cases: when we consider all bounding boxes, when we leave out bounding boxes in the ends of the pool (i.e. the first 5 meter and last 5 meter), and finally do the latter again for each separate lane.

Object-based metrics are based on the complete laps of each swimmer. The failure rate of the algorithm is measured by counting the number of manual interactions needed to identify every lap of a given swimmer as a single, continuous track. A single interaction is defined as the connection of one track fragment to another. Note that this definition does not include the number of interactions required to decide which fragments to connect. For an operational system a user could interact with the system to connect two track fragments using a maximum of two mouse clicks (selecting the end point of one track and the starting point of the other track) but examination of the video clip may be needed to decide which fragments to connect. After the complete laps have been identified for each swimmer, with manual correction if necessary, the measured lap times are compared to the ground truth.

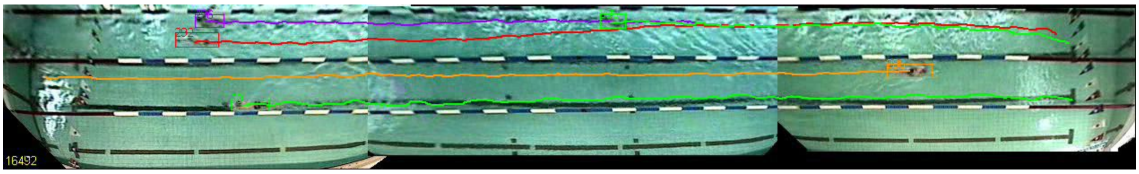

Figure 8. The visualization output of the tracking result. Each swimmer is represented by a bounding box with its track over time.

Table 1. The detection performance of our tracking method measured by the frame-based metrics.

	# True Positives	# False Positives	# False Negatives	Tracker Detection Ratio	False Alarm Rate
All lanes	3328	250	1153	0,74	0,07
All lanes excluding pool ends	3094	250	199	0,94	0,07
Lane 1 (lower) excluding pool ends	238	22	23	0,91	0,08
Lane 2 (middle) excluding pool ends	1023	25	54	0,95	0,02
Lane 3 (upper) excluding pool ends	1819	220	132	0,93	0,11

Results & Discussion

Setting up the mobile data acquisition system took about 40 minutes. Care had to be taken to position the cameras correctly in order to achieve the right degree of overlap between the 3 views. During data processing a total of 12 points in the 3 views had to be selected manually to register the images correctly. The prototype contains no mechanism to ensure that the camera position and viewing are repeatable between training sessions and within training sessions the camera positions can move if the tripods or the connecting wires are accidentally displaced, forcing recalibration of the system. In general, the more variable the camera and scene geometry is the higher the burden on the computer vision algorithm and these factors favor the use of multiple fixed acquisition systems at different locations rather than a single mobile system.

Figure 8 shows an example of the tracking algorithm output. The detection performance measured for 45 minutes of video using frame-based metrics is presented in Table 1. For all swimmers in all lanes the tracker detection ratio is 0.74 and the false alarm rate is 0.07. Many of the false negatives are caused by the swimmers at the ends of the pool: when bounding boxes within 5 meters from the pool ends are excluded from the analysis the detection ratio improves to 0.94 and the false alarm rate remains 0.07. The reason for this is that swimmers at the ends of the pool are often resting or underwater, meaning that their motion or color properties are less distinguishable from their environment. If the pool ends are excluded and the different lanes are compared, the best results are obtained from lane 2. In lane 3 the relatively high false alarm rate is due to bright reflections, caused by light entering from a window on the other side of the pool, that are sometimes mistaken for swimmers. The lower tracker detection ratio in lane 1 is due to imperfect calibration of the setup which causes the swimmer to partly fall outside the view and be undetected by the prototype system.

Figure 9 shows examples of 4 failure modes for the detection algorithm. Many of the false negatives reported above are caused by a failure to detect swimmers at the ends of the pool when they are resting (Figure 9a) or underwater (Figure 9b). In addition, water waves can cause false negatives by covering the swimmer (Figure 9c) and water reflections can cause false positives (Figure 9d).

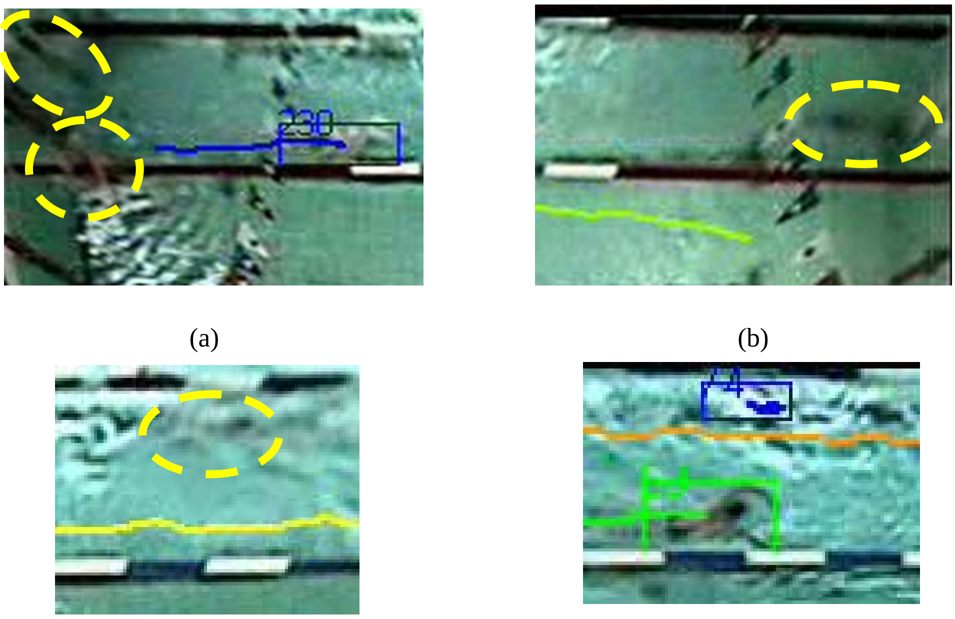

(a) (b) (c) (d)

Figure 9. The types of difficulty encountered during the whole training registration process (best viewed in color): (a) Resting swimmers and (b) swimmers underwater could not be detected (shown here with yellow dashed circles), (c) water reflections and water ripples caused misdetection (undetected swimmer within yellow dashed circle) and (d) false detection (upper rectangle).

Table 2. Comparison of the number of manual interactions needed in three stages during the track repair method.

		Number of laps in Ground Truth set	Number of manual interactions needed		
			Before track repair	After grouping fragmented tracks	After grouping laps to swimmers
Lane 1	Swimmer 1	23	75	22	0
Lane 2	Swimmer 2	54	131	53	6
	Swimmer 3	51	57	50	6
Lane 3	Swimmer 4	52	132	51	27
	Swimmer 5	53	98	52	28
	Swimmer 6	58	104	57	17
	Swimmer 7	47	99	46	17
	Total	338	696	331	101

Table 2 shows the number of manual interactions needed to correctly identify the complete laps of each swimmer. Before track repair an average of 100 manual interactions per swimmer would be required to correct the results because the tracks of individual laps are fragmented. After automatically grouping fragmented tracks each lap is represented by a single track, but laps have not been associated to swimmers (See Figure 10). After grouping laps to swimmers the system is not able to solve instances when two or more swimmers are resting at the same end of the pool. These situations are recognized by the algorithm but have to be resolved manually. They never occur in lane 1 which is occupied by a solitary swimmer and often occur in lane 3 which is shared by four swimmers. After all tracking methods have been applied the number of manual interactions required for correct swimmer tracking is at best none and at worst 28 depending on which swimmer is tracked. Note that trials showed that no manual interactions were necessary to accurately track the swimmers in lane 2 if the algorithm made use of the fact that each swimmer used only one half of the lane and the vertical position was used for inter-lap track repair. For elite athletes this constraint usually applies because it most closely matches race behavior.

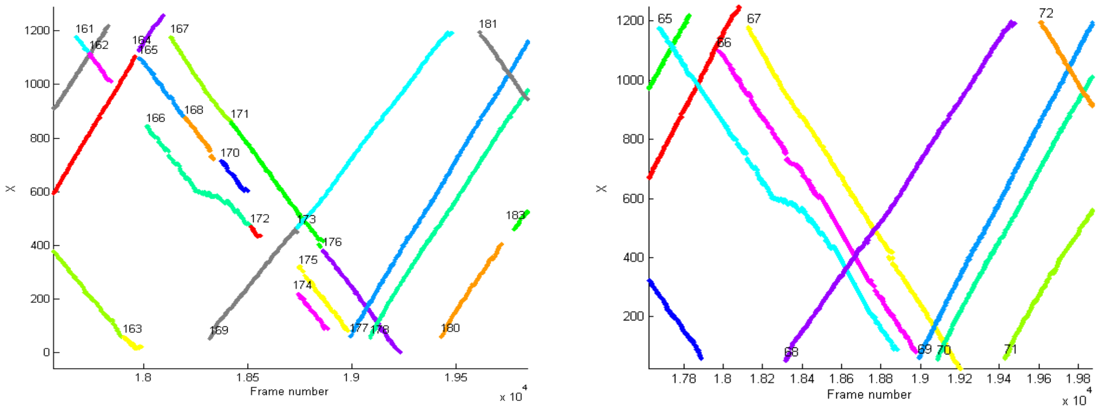

(a) (b)

Figure 10. (a) The visualization of the fragmented tracks (best viewed in color). Each line segment is a collection of centre of gravity points of the detected swimmer blobs. The segments are drawn here using only the x coordinate of the centre points and the frame numbers (time axis). Upward lines in time represent swimmers going from left to right. In the matching, the y coordinate is also considered. For example, segment 172 (red) should be matched to segment 174 (magenta). Without using the extrapolation, segment 172 would have been matched to segment 175 (yellow), which has the same direction and is the closest. (b) The results after grouping the fragmented tracks. The gaps between tracks are now filled with interpolated values.

Table 3. Results from the object-based evaluation: statistics of the elapsed time discrepancy and the average speed discrepancy.

	Elapsed time discrepancy (after repair)	
	Mean (sec)	Standard Deviation (sec)
Swimmer 1	2,62	1,61
Swimmer 2	1,69	2,33
Swimmer 3	0,52	0,60
Swimmer 4	2,04	2,08
Swimmer 5	1,29	2,35
Swimmer 6	0,43	0,74
Swimmer 7	1,57	1,74

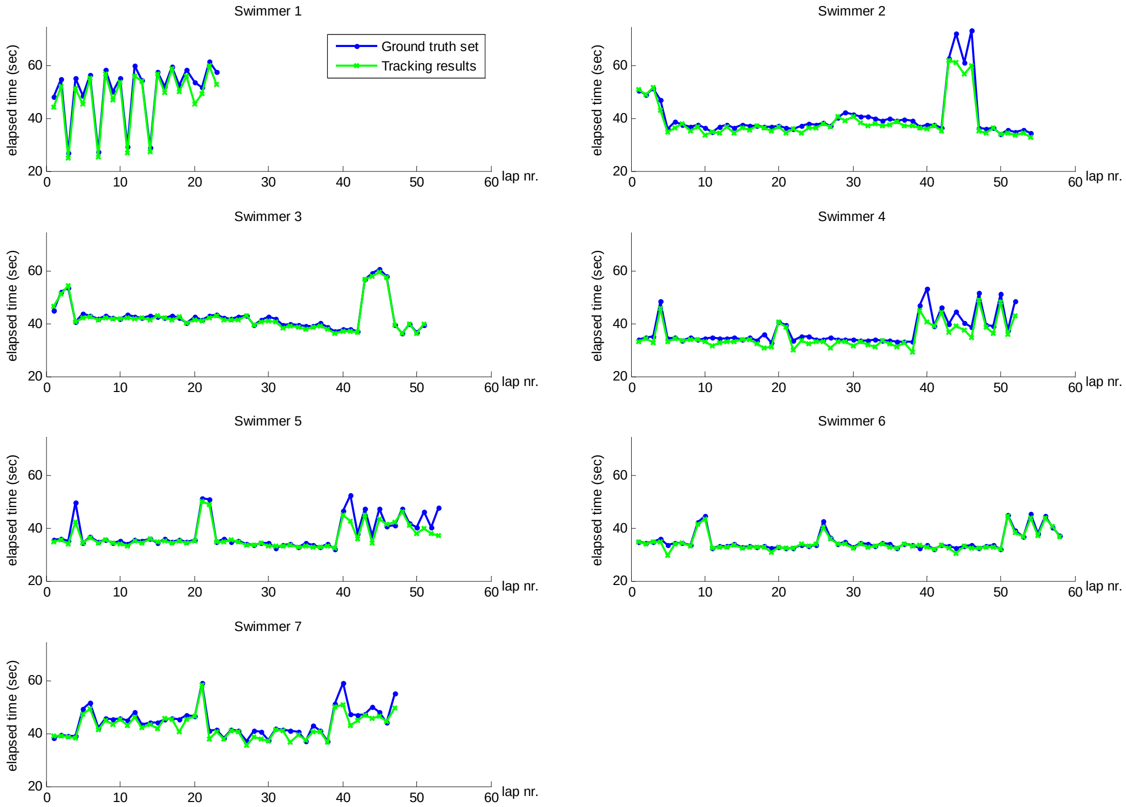

Figure 11. The elapsed time plots for all laps of all swimmers. The ground truth lap times (blue) are compared to the tracking results (green) after manual correction. Patterns dictated by the training schedule can be discerned in these plots, for example, swimmer 1 swims with a pattern of a few slow laps and 1 fast lap during the first 15 laps.

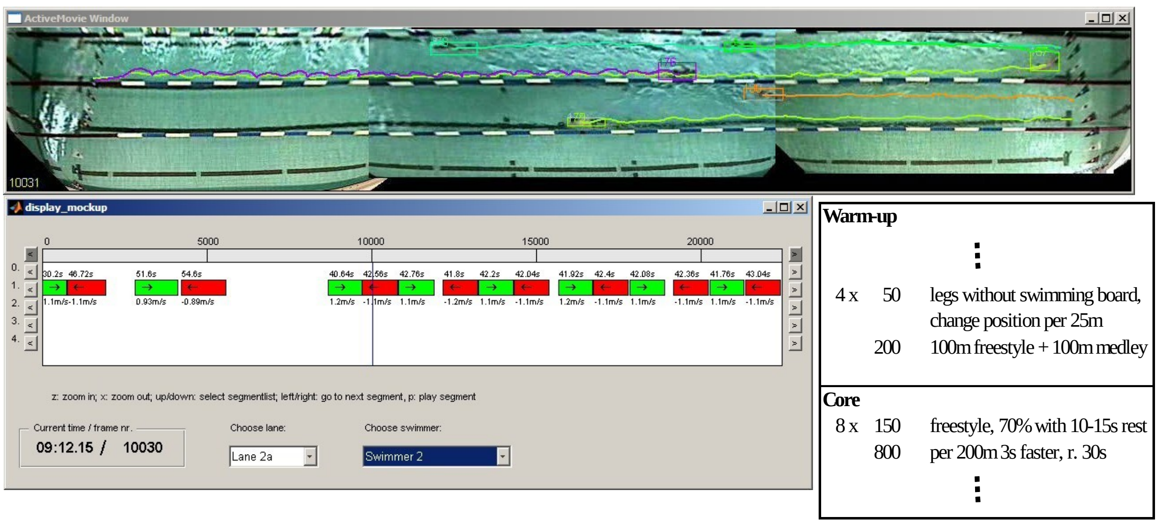

Figure 12. Comparison of the registered laps of a swimmer to the training schedule. This part shows the performance of swimmer 3 (upper halve middle lane) during the transition between warm-up and core training. Note that each segment in the visualization represents a 50m lap and the swim direction is indicated by different segment colors.

The lap times of all swimmers are depicted in Figure 11. The mean and the standard deviation of the measurement discrepancies are summarized in Table 3. The measurement discrepancy is defined as the estimated value subtracted from the ground truth value. The mean discrepancy for the lap time measurements is typically 4% of the lap time. It can be seen from Table 3 that the automatically-measured lap times are systematically shorter than the true lap times, sometimes with a significant difference when swimmers move slowly. This is mainly caused by the failure of the algorithm to initialize tracks at the moment the swimmers start a lap. At the start of a lap, the swimmers are often underwater after completing a tumble-turn and may not be detected until they have moved several meters from the pool wall and resurfaced (see Figure 8). Trials indicated that linearly extrapolating the tracks to the pool edge using the average speed of the first 4 seconds of each track improved the lap time estimates but that linear interpolation is not optimal because swimmers show a tendency to go faster at the beginning of a lap.

To allow a coach to check that a swimmer has completed a training session as instructed it is necessary to map the written training schedule to the system output. It has been found that the registered laps show patterns that can make this possible and this issue will be the subject of future work. Figure 12 shows an example of a swimmer swimming the last 2x100m of a warm-up, taking a rest, and beginning the core training by swimming groups of 150m (3 laps) with 10-15 seconds rest in between.

Conclusions and Future Work

We have described results from a prototype system designed to register the training sessions of swimmers using video recordings. These results allow us to draw conclusions about design requirements for future systems and likely performance limitations.

Regarding video acquisition hardware we have observed that the mobile prototype requires time and specialist knowledge to assemble and that changes in the scene and camera geometry will be source of variability in the system performance. We conclude that fixed systems are likely to offer advantages over mobile systems in terms of data quality and repeatability of results. For mobile systems a simpler set-up with fewer cameras and easier assembly and calibration would be advantageous.

Regarding computer vision techniques we have shown that, although joining laps is difficult, it is possible to track each lap swum by 7 swimmers taking part in a 45 minute training session automatically using a simple background modeling and blob tracking method. Many difficulties encountered during tracking, such as intra-lap track fragmentation and inter-lap track association can be corrected by using constraints about the swimmers motions, which are predictable and repetitive. The main limitation on the algorithm performance is the failure to detect swimmers at the ends of the pool that are either resting or underwater. The failure to detect resting swimmers means that manual interactions are necessary to distinguish between swimmers who take a rest together at the same end of the pool. The failure to detect swimmers swimming underwater after tumble turns causes lap times to be systematically underestimated by typically 1.5 seconds. The tracking output shows patterns of laps and pauses that can make it possible to manually map the written training schedule of the coach to the system output to obtain an overview of the training session as performed.

Our results show that the performance of the system can be highly dependent on the way in which the swimmers behave and how the training sessions are organized. For example, much more manual interaction is necessary to correct the tracking results when swimmers rest together at the same end of the pool or share the same swim lane and swim in a circulating pattern rather than swimming backwards and forwards in the same part of the lane. One way to improve the performance of the system without further algorithm development is for the training sessions to be organized in a way that avoids these situations and develop guidelines for the coaches and swimmers. The use of colored swim caps could also improve the segmentation performance at the ends of the pool and allow swimmer positions and identities to be tracked more accurately.

Acknowledgements

This research is supported by the BSIK-project MultimediaN and is made possible by the collaboration with NOC*NSF, the Dutch Olympic Committee and National Sport Federation. The authors would like to thank the reviewers for their useful comments and suggestions.

References

Bashir, F. & Porikli, F. (2006). Performance Evaluation of Object Detection and Tracking Systems. *Proceedings of IEEE International Workshop on Performance Evaluation of Tracking and Surveillance*, 7-14.

Baumberg, A.M. & Hogg, D. (1995). An Adaptive Eigenshape Model. *Proceedings of the Sixth British Machine Vision Conference, vol. 1*, 87-96.

Bouguet, J.-Y. (2006). Camera Calibration Toolbox for MATLAB, http://www.vision.caltech.edu/bouguetj/calib_doc/index.html [02.11.2006].

Dartfish (2006), Dartfish Video Software Solutions, http://www.dartfish.com [02.11.2006].

Davies, E.R. (2005). *Machine Vision: Theory, Algorithms, Practicalities*. San Fransisco: Morgan Kaufmann Publishers.

Doermann, D. & Mihalcik, D. (2000). Tools and Techniques for Video Performance Evaluation. *Proceedings of the International Conference on Pattern Recognition*, 4167-4170. http://sourceforge.net/projects/viper-toolkit/ [02.11.2006].

Eng, H.-L., Wang, J., Wah, A.H.K.S. & Yau, W.-Y. (2006). Robust Human Detection within a Highly Dynamic Aquatic Environment in Real Time. *IEEE Transactions on Image Processing*, *15(6)*, 1583-1600.

Elgammal, A., Duraiswami, R., Harwood, D. & Davis, L.S. (2002). Background and Foreground Modeling using Non-parametric Kernel Density Estimation for Visual Surveillance. *Proceedings of the IEEE*, *90(7)*, 1151-1163.

Gavrila, D.M. & Philomin, V. (1999). Real-time Object Detection for Smart Vehicles. *Proceedings of IEEE International Conference on Computer Vision*, 87-93.

Hu, W., Tan, T., Wang, L. & Maybank, S. (2004). A Survey on Visual Surveillance of Object Motion and Behaviors. *IEEE Transactions on Systems, Man, and Cybernetics–Part C: Applications and Reviews*, *34(3)*, 334-352.

Nguyen, H.T. & Smeulders, A.W.M. (2004). Tracking Aspects of the Foreground against the Background. *Proceedings of European Conference on Computer Vision*, 446-456, LNCS 3022.

Perše, M., Kristan, M., Perš, J., & Kovačič, S. (2006). A Template-based Multi-Player Action Recognition of the Basketball Game. *Proceedings of ECCV Workshop on Computer Vision Based Analysis in Sports Environments*, 71-82.

Stauffer, C. & Grimson, W.E.L. (1999). Adaptive Background Mixture Models For Real-time Tracking. *Proceedings of IEEE Conference on Computer Vision and Pattern Recognition*, *2*, 245-252.

STR (Swimming Technology Research) (2006). Aquanex for Improving Performance, http://swimmingtechnology.com/aquanex.htm [02.11.2006].

Urtasun, R., Fleet, J.F. & Fua, P. (2005). Monocular 3–D Tracking of the Golf Swing. *Proceedings of IEEE Conference on Computer Vision and Pattern Recognition*, *2*, 932-938.

Viola, P., Jones, M.J. & Snow, D. (2005). Detecting Pedestrians Using Patterns of Motion and Appearance. *International Journal of Computer Vision*, *63(2)*, 153-161.

Wang, J.R. & Parameswaran, N. (2004). Survey of Sports Video Analysis: Research Issues and Applications. *Proceedings of Pan-Sydney Area Workshop on Visual Information Processing*, *36*, 87-90.

Xu, M., Orwell, J. & Jones, G. (2004). Tracking Football Players with Multiple Cameras. *Proceedings of IEEE International Conference on Image Processing*, 2909-2912.

A Computerized Dynamic Synthesis Method for Generating Human Aerial Movements

F. Leboeuf, G. Bessonnet, P. Lacouture

Laboratoire de Mécanique des Solides, CNRS-UMR 6610, Université de Poitiers, SP2MI, Bd. M. & P. Curie, BP 30179, 86960 Futuroscope Chasseneuil Cedex, France)

Abstract

A computerized method based on optimal dynamic synthesis was developed for generating the flight phase of somersaults. A virtual gymnast is modeled as a planar seven-segment multibody system with six internal degrees of freedom. The aerial movement is generated using a parametric optimization technique. The performance criterion to be minimized is the integral quadratic norm of the torque generators. The method produces realistic movements showing that somersaults perfectly piked or tucked appear spontaneously according to the value of the rotation potential of the initial movement. It provides accurate knowledge of the evolution of joint actuating torques controlling the somersault, and makes it possible to investigate precisely the configurational changes induced by modifications of the rotation potential. Four simulations are presented: one with a reference value for the rotation potential, two with reduced values, and the last with a different hip flexion limit. They give an insight into the coordination strategies which make the movement feasible when the rotation potential is decreased. The method gives accurate assessments of the energetic performance required, together with precise evaluations of the mechanical efforts to be produced for generating the acrobatic movement

KEY WORDS: AERIAL MOVEMENT; DYNAMIC SYNTHESIS; OPTIMIZATION; MOVEMENT GENERATOR

Introduction

Human aerial movements performed in gymnastics and in sport acrobatics such as diving, ski jumping, tumbling and trampolining comply with subtle dynamic effects that athletes and gymnasts must perceive and control. Better understanding of the intrinsic dynamics of such movements may be achieved through experimental assessments and numerical simulations. A variety of approaches based on dynamic modeling were proposed in the literature to get deeper insight into the way somersaults could be initiated and controlled.

A general idea consists of developing computerized simulations models adjusted to experimental data in order for the movements simulated to match at best their actual counterparts performed by gymnasts (Yeadon & Mikulcik, 1996; Requejo et al., 2002; Yeadon & King, 2002). In Yeadon & Mikulcik (1996), a specific approach exploits directly the distinctive nature of aerial movements which are characterized by the absence of external contact and the subsequent conservation of angular momentum about the centre of mass of the biomechanical system. The authors take advantage of this condition to design computer simulation models in which conservation relationships are dealt with so as to compute time histories of three angles defining the body orientation assuming that time histories of joint angles defining the body configuration are known.

Developing models suited to simulating observed aerial movements, and assessing experimentally their accuracy, was also a main concern in recent years (Requejo *et al*., 2002; Yeadon & King, 2002). Different methods were developed to achieve this aim. An approach is based on using control models of movement in order to compensate for errors produced by inverse dynamics (Requejo *et al*., 2002). Differently, development and evaluation of a simulation model can be carried out using matching optimization procedures as in Yeadon & King (2002).

Above mentioned approaches are concerned with fitting subject-specific simulation models to observed movements. They incorporate kinematic data derived from recorded movements. This allows for solving inverse dynamic problems. In Blajer & Czaplicki (2001), this method is used to compute actuating moments generated at joints during both the support phase and the flying phase of somersaults performed on trampoline. The estimation of actuating torques provides key information on the way intersegmental movements were coordinated and controlled. It may help gymnasts and trainers to better analyze inner dynamics of somersaults in order to improve their execution.

This paper presents another way to investigate the intrinsic dynamics of aerial movements such as somersaults. It is based on a dynamic synthesis approach. The method presented offers new possibilities for simulating aerial movements. Its main characteristic lies in the fact that the simulation problem is freed from time histories of any variables such as orientation angles which describe the evolution of body configurations, and the torque generators which control the joint movements. Thus, as experimental data defined along the motion time is not required, numerical simulations combine body inertia, movement kinematics and actuating moments exactly. This makes it possible to accurately analyze internal dynamics of fast aerial movements. However, it should be noted that the numerical simulations carried out are not aimed at mimicking closely real somersaults performed by gymnasts. The objective is to reveal how a human-like aerial movement may be self-organized in a natural way when its basic parameters are modified.

Methods

Somersaults tucked or piked are basic exercises in sport acrobatics and gymnastics. As for any aerial movement, the athlete play consists of modulating his configuration changes during flight in order to generate desired rotational effects. We consider non twisting somersaults in order to get a clear insight into the way changes in dynamic data have an effect on the kinematic characteristics of the movement.

Kinematic model

The movement can be described in the athlete sagittal plane which is assumed to remain vertical. Thus, a planar model made of seven rigid body-segments as depicted in figure 1 was accounted for. It is similar to the model taken into account in Blajer & Czaplicki (2001) for a gymnast performing trampoline jumps.

Nine generalized coordinates are required to describe the movement of this multibody model in a fixed vertical plane. Two of them may be the Cartesian coordinates x and y of the center of mass G of the whole body:

$$\mathbf{OG} = x\mathbf{X}_0 + y\mathbf{Y}_0, \qquad (1)$$

where $\mathbf{X}_0$ and $\mathbf{Y}_0$ are orthogonal unit vectors of horizontal and vertical directions in the vertical movement plane.

The next coordinates, each one defined as the oriented angle between the fixed reference vector $\mathbf{X}_0$ and the vector $\mathbf{X}_i$ attached to the link L_i, such that:

$$q_i = (\mathbf{X}_0, \mathbf{X}_i),\ 3 \le i \le 9, \qquad (2)$$

describe the absolute rotations of body segments $L_i s$ (Figure 1). We will also use the vector representations:

$$\mathbf{q} = (q_3,...,q_9)^T,\ \ \dot{\mathbf{q}} := \partial\mathbf{q}/\partial t,\ \ \ddot{\mathbf{q}} := \partial^2\mathbf{q}/\partial t^2.$$

It should be noted that the six joint angles θ_i defined using (2) as:

$$\begin{cases} \theta_i = q_i - q_{i-1}\ ,\ 4 \le i \le 9,\ i \ne 7 \\ \theta_7 = q_7 - q_3 \end{cases}, \qquad (3)$$

together with any absolute rotational angle chosen among the $q_i s$, for instance q_3, could be used equivalently to describe all rotational movements. However, dynamic modeling of a planar movement is by far more concise using absolute body-segment rotations than joint coordinates. Thus, angles $\theta_i s$ will be used only in (11) below for a clear representation of joint movement limitations.

Most often, somersaults are performed using springboards, trampolines or tumbling floor at takeoff. In order to prevent too large variable initial conditions, we consider somersaults performed on stiff floor. In this way, the velocity of the foot tip A_9 in figure 1 must be equal to zero at takeoff. This assumption will make it possible to adjust optimally initial joint velocities with respect to a given value of angular momentum while avoiding that lower body segments gain initial momentum from the ground, which could be quite variable from one simulation to another.

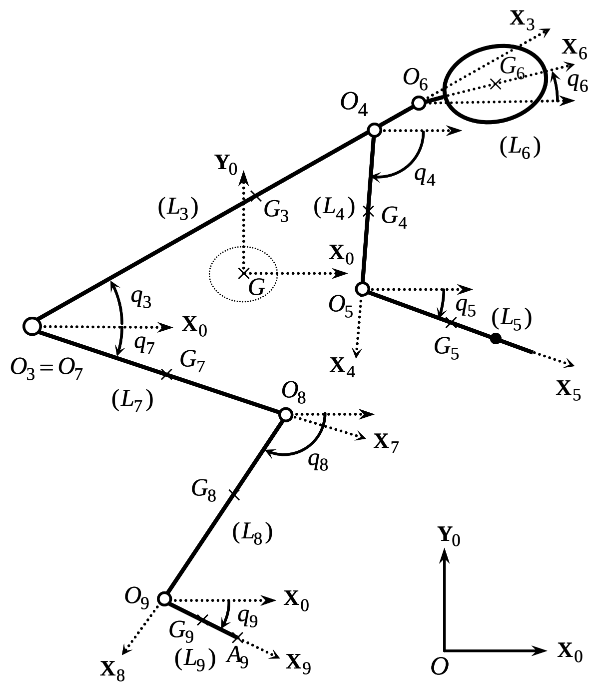

Figure 1. Sagittal kinematic model of a gymnast performing a somersault

Dynamic model

During the aerial phase, the center of mass G describes a ballistic parabola whose characteristics are determined by initial conditions at takeoff. This translational movement can be dissociated from rotational movements of the mechanical system. A classical approach consists of describing the rotational movements in Koenig's frame $(G;\mathbf{X}_0,\mathbf{Y}_0)$ (represented in dotted lines in Figure 1) which remains in translation in the inertial frame, and with origin at the center of mass G of the mechanical model.

First, let us consider Newton's equation and Euler's equation for the whole system. They result in the two relationships

$$\dot{\mathbf{V}}^0(G) = \mathbf{g}\,, \tag{4}$$

$$H^0(\mathbf{q},\dot{\mathbf{q}}) = cste\,, \tag{5}$$

respectively. The first expresses that the acceleration $\dot{\mathbf{V}}^0(G)$ of G (time derivative of the velocity vector $\mathbf{V}^0(G)$) with respect to the inertial frame $(O;\mathbf{X}_0,\mathbf{Y}_0)$ (the superscript "0" in (4) and (5) refers to this frame) is equal to the gravity acceleration **g**. The second means that the total angular momentum $H^0(\mathbf{q},\dot{\mathbf{q}})$ about the central axis $(G;\mathbf{Z}_0)$ $(\mathbf{Z}_0 = \mathbf{X}_0 \times \mathbf{Y}_0)$ remains constant during the aerial movement. This first order equation will be considered as a constraint relationship to be satisfied by $\mathbf{q}$ and $\dot{\mathbf{q}}$ (Section 2.4, equation (20)).

Second, referring to Koenig's frame, one can write for any point P of the mechanical system (the superscript "K" below refers to this frame):

$$\dot{\mathbf{V}}^0(P) = \dot{\mathbf{V}}^K(P) + \dot{\mathbf{V}}^0(G)\,.$$

Using (1), this relationship may be considered as

$$\dot{\mathbf{V}}^K(P) = \dot{\mathbf{V}}^0(P) - \mathbf{g}\,.$$

It shows that accelerations computed in Koenig's frame result from subtracting the gravity acceleration from absolute accelerations. This simple result has the well known consequence: when the Newton-Euler equations for movements of free systems are formulated in Koenig's frame, the gravity acceleration vanishes (This remark applies to Lagrange's equations as well). On the other hand, as we need an inverse dynamic model for implementing the parametric optimization technique we have in mind, we chose to use Newton-Euler equations. This approach simplifies the relationships needed. Furthermore, the dynamic model may be derived using the very efficient recursive algorithm from Luh et al. (1980) of which computational complexity increases just linearly with the number of degrees of freedom. It provides six independent relationships defining the six torque generators τ_i we expressed formally as the following functions of $\mathbf{q}$, $\dot{\mathbf{q}}$ and $\ddot{\mathbf{q}}$ (see part A2 of the Appendix for details):

$$t \in [t^i, t^f]\,,\ \tau_i(t) = f_i(\mathbf{q}(t),\dot{\mathbf{q}}(t),\ddot{\mathbf{q}}(t))\,, 4 \le i \le 9\,, \tag{6}$$

where t^i and t^f represent given initial time and final time of the movement. Each torque τ_i is exerted at O_i by the adjacent link L_j on link L_i, with $j \le i-1$.

Stating a dynamic optimization problem

The objective to be reached consists of extracting a solution $t \to (\boldsymbol{\tau}(t),\mathbf{q}(t))$ from equations (5) and (6), by minimizing a dynamic cost while satisfying a set of constraints as stated below. Two distinctive criteria are generally used for generating optimal movements of controlled multibody systems: the minimum energy cost and the minimum effort cost. The former generates discontinuous control variables of bang-off-bang type (Leboeuf et al., 2006). The latter has the effect of attenuating the peak values of the torques generators while ensuring good stress spread between all active joints. Thus, the criterion we have chosen to minimize is the integral quadratic morn of joint actuating torques

$$J = \int_{t^i}^{t^f} \boldsymbol{\tau}(t)^T \boldsymbol{\tau}(t)\, dt \tag{7}$$

The criterion (7) will act as an organizing principle for the simulated movements, having the ability to determine an optimal way of combining dynamic loads due to inertia of body segments with joint driving torques that create the movement.

Somersaults to be generated are characterized by specific conditions they must obey. First, information on initial and final conditions is required. Initial configuration at takeoff and final configuration at touch-down were estimated from video analysis of somersaults performed by an expert gymnast. Thus, we define the two seven-order vector-constraints

$$\begin{aligned} &\Phi_1(\mathbf{q}(t^i)) := \mathbf{q}(t^i) - \mathbf{q}^i = 0 \ (\in \Re^7), \\ &\Phi_2(\mathbf{q}(t^f)) := \mathbf{q}(t^f) - \mathbf{q}^f = 0 \ (\in \Re^7), \end{aligned} \tag{8}$$

where the values of vectors $\mathbf{q}^i$ and $\mathbf{q}^f$ are given data.

Initial and final joint velocities are unspecified. However, initial velocities $\dot{q}_k(t^i)$, $k \in \{3,...,9\}$, must comply with the condition anticipated in section 1.1, expressed as

$$\mathbf{V}^0(A_9) = 0 .$$

Considering Koenig's frame, the vector velocity in the left hand member is correlated to the velocity of G by the formula

$$\mathbf{V}^0(A_9) = \mathbf{V}^K(A_9) + \mathbf{V}^0(G) ,$$

which results in

$$\mathbf{V}^K(A_9) + \mathbf{V}^0(G) = 0 ,$$

where $\mathbf{V}^K(A_9)$ may be expressed formally as the function of $\mathbf{q}(t^i)$ and $\dot{\mathbf{q}}(t^i)$:

$$\mathbf{V}^K(A_9) = \Psi_{A_9}(\mathbf{q}(t^i), \dot{\mathbf{q}}(t^i)) .$$

Similarly, the initial velocity of G can be defined through (1) as the vector function

$$\Psi_G(\dot{x}^i, \dot{y}^i) := \mathbf{V}^0(G) = \dot{x}^i \mathbf{X}_0, + \dot{y}^i \mathbf{Y}_0 ,$$

where the components $\dot{x}^i$ and $\dot{y}^i$ are correlated to the flight time of the somersault. They will be considered as given data. Finally, representing kinematic conditions at takeoff by the function

$$\Phi_3(\mathbf{q}(t^i), \dot{\mathbf{q}}(t^i)) := \Psi_{A_9}(\mathbf{q}(t^i), \dot{\mathbf{q}}(t^i)) + \Psi_G(\dot{x}^i, \dot{y}^i) = 0 \,(\in \Re^2) , \tag{9}$$

we put together constraints (8) and (9) into the 16-dimensional vector-function:

$$\Phi = (\Phi_1^T, \Phi_2^T, \Phi_3^T)^T ,\ \Phi(\mathbf{q}(t^i), \mathbf{q}(t^f), \dot{\mathbf{q}}(t^i)) = 0 \ (\in \Re^{16}) . \tag{10}$$

Moreover, state constraints limiting joint rotations must be taken into account in order to respect human movement limitations, such as avoiding hyperextensions. Using relative joint rotations as defined in (3), such constraints are simply represented by the set of double inequalities

$$\theta_k^{\min} \le \theta_k(\mathbf{q}) \le \theta^{\max} .$$

They will be dealt with as the double set of one-sided constraints

$$t \in [t^i, t^f], 4 \le k \le 9, \begin{cases} h_k(\mathbf{q}(t)) := \theta_k^{\min} - \theta_k(\mathbf{q}(t)) \le 0 \\ h_{k+6}(\mathbf{q}(t)) := \theta_k(\mathbf{q}(t)) - \theta_k^{\max} \le 0 \end{cases}, \quad (11)$$

abridged by setting

$$\mathbf{h} = (h_1,...,h_{12})^T,\ t \in [t^i, t^f],\ \mathbf{h}(\mathbf{q}(t)) \le 0\ (\in \Re^{12}). \quad (12)$$

To end with, the dynamic optimization problem to be solved can be summarized as follows: find a double-vector time-varying function $t \to (\boldsymbol{\tau}(t), \mathbf{q}(t))$ solution of (5) and (6), minimizing (7), and satisfying the constraints (10) and (12). This is typically an optimal control problem with $t \to \boldsymbol{\tau}(t)$ as control variable, and $t \to \mathbf{q}(t)$ as state variable.

A variety of computational techniques could be used to solve this problem. However, optimal control problems stated in the field of multibody system dynamics are prone to stiff computational behavior. Implementation of a parametric optimization technique offers an efficient means to overcome this problem.

Parametric optimization technique

Parameterizing an optimal control problem may be achieved using different approaches. The reader is referred to Hull (1997) for a brief presentation of possible conversions of optimal control problems into parametric optimization problems. Further valuable information on this issue is also available in the survey (Ren et al., 2006). Intrinsically, parameterization techniques are derived from approximating control variables and/or state variables using a finite set of discrete parameters to be varied in order to solve approximately the initial optimization problem. A first method is based on approximating the control variables. This approach was used notably in Pandy et al. (1992) and Anderson & Pandy, (2001) to generate optimal movements using musculoskeletal models of the human locomotion system. As integration of dynamics equations is required, an initial state of the system is needed.

In contrast, parameterizing the state variables makes it possible to deal simply with constrained initial state as defined by (9), and partly unspecified in order to be optimized. This second method was noticeably developed by Bobrow et al. (2001) for generating robot motions and human movements. In a similar way, Lo et al. (2002) outlined a general approach to formalize and convert optimal human motion-planning into a state-based parametric-optimization problem. In both above references, this transformation is based on the discretization of the generalized coordinates q_is of the movement using cubic Bsplines of class C^2 (twice continuously differentiable).

We adopted a somewhat different approach which makes use of smoother approximating functions than the previous ones. It can be summarized as follows.

First, the interval of time is split up into *N* equal subintervals I_k defined as

$$\begin{cases} t^i = t_1 \le ... \le t_k \le ... \le t_{N+1} = t^f, \\ I_k = [t_k, t_{k+1}],\ t_{k+1} - t_k = (t^f - t^i)/N. \end{cases} \quad (13)$$

Next, configuration variables q_is are approximated by known time-functions ϕ_is depending on shaping parameters which are the values of the q_is themselves at junction times (or nodes) t_k, plus, in the present case, their first-order derivatives at initial time, such that

$$3 \le i \le 9, \begin{cases} q_i(t) \cong \phi_i(X^i, t), \\ X^i = (\dot{q}_i(t_1), q_i(t_1), q_i(t_2), ..., q_i(t_{N+1})). \end{cases} \quad (14)$$

As in Seguin & Bessonnet (2005), we used spline functions of class C^3 as approximating functions ϕ_is . They are the concatenation of 4-order polynomials defined on the subintervals I_k, and linked successively at nodes t_k up to their third derivative. This high order of smoothness is required to avoid jerky accelerations and to allow the constraints to be accurately satisfied.
At this point, setting

$$X = ((X^3)^T,...,(X^9)^T)^T, \quad \boldsymbol{\varphi}(X,t) = (\phi_3(X^3,t),...,\phi_9(X^9,t))^T, \tag{15}$$

the configuration vector $\mathbf{q}$ is properly approximated by the parameterized vector-function $\boldsymbol{\varphi}$ such that

$$t \in [t^i, t^f], \ \mathbf{q}(t) \cong \boldsymbol{\varphi}(X,t). \tag{16}$$

It follows that, through equation (6) and representation (16), the vector $\boldsymbol{\tau}$ of torque generators can be approximated by the function $\boldsymbol{\tau}^*(X,t)$ defined by setting

$$\boldsymbol{\tau}(t) \cong \boldsymbol{\tau}^*(X,t) := f(\boldsymbol{\varphi}(X,t), \frac{\partial \boldsymbol{\varphi}}{\partial t}(X,t), \frac{\partial^2 \boldsymbol{\varphi}}{\partial t^2}(X,t)). \tag{17}$$

Then, the criterion J is approximated by the function $F(X)$ such that

$$J \cong F(X) := \int_{t^i}^{t^f} \boldsymbol{\tau}^*(X,t)^T \boldsymbol{\tau}^*(X,t) dt. \tag{18}$$

It should be noticed that equation (6) is embedded in the construction of $F(X)$ in (18) through the expression of $\boldsymbol{\tau}^*$ in (17). Therefore, only the conversion of equation (5) and constraints (10) and (11) still remains to be done. Using the representation (16), these constraints can be approximated using new functions Φ^* , H^* and $\mathbf{h}^*$, defined as

$$\Phi^*(X,t^i,t^f) \cong \Phi(\boldsymbol{\varphi}(X,t^i), \boldsymbol{\varphi}(X,t^f), \frac{\partial \boldsymbol{\varphi}}{\partial t}(X,t^i)) = 0, \tag{19}$$

$$H^*(X,t) \cong H^0(\boldsymbol{\varphi}(X,t), \frac{\partial \boldsymbol{\varphi}}{\partial t}(X,t)) - H^0(t^i)) = 0, \tag{20}$$

$$\mathbf{h}^*(X,t) \cong \mathbf{h}(\boldsymbol{\varphi}(X,t)) \le 0. \tag{21}$$

In (20), $H^0(t^i)$ represents the given value of angular momentum gained at takeoff. The running time t must be eliminated from constraints (20) and (21) in order to achieve the conversion of the original problem into a parametric optimization problem. A simple approach is based on taking into account these constraints at nodes t_k only. Preliminary numerical tests showed that slight infringements may appear between nodes. Small violations of configuration constraints (21) are acceptable. On the other hand, any minor oscillation of the angular momentum has the effect of generating odd movements. Thus, the constraint (20) needs to be accurately satisfied along the movement time. A means to ensure this requirement is based on implementing a penalty technique. It consists of minimizing the total constraint violation. We extend this approach to inequality constraints (21) by considering the constraint infringements defined as

$$h_k^{*+}(X,t) = Max(h_k^*(\boldsymbol{\varphi}(X,t),0); \ \mathbf{h}^{*+} = (h_1^{*+},...,h_{12}^{*+})^T.$$

Then, the method results in minimizing the augmented algebraic cost

$$F^*(X) = F(X) + \int_{t^i}^{t^f} [r_1 H^*(X,t)^2 + r_2 (\mathbf{h}^{*+}(X,t))^T \mathbf{h}^{*+}(X,t)] dt, \tag{22}$$

where r_1 and r_2 are given penalty factors. The greater they are, the smaller the residual values of penalty functions in the integral will be after minimization.

The final problem may be reformulated as follows: for reasonably great values of r_1 and r_2, minimize the cost function F^* in (22) subjected to constraint (19). This minimization problem of non linear programming was solved using the routine *fmincon* of the Matlab® Optimization Toolbox, which implements Sequential Quadratic Programming algorithms.

Let us mention that in the numerical simulations carried out, both values of r_1 and r_2 were set at 1000. The resulting maximum residual value of the angular momentum H^0 amounted to 0.04$kg.m^2.s^{-1}$ (0.08% of the nominal value set at 40 $kg.m^2.s^{-1}$) with a standard deviation of 0.007$kg.m^2.s^{-1}$. On the other hand, the time interval $[t^i, t^f]$ was divided into sixteen subintervals (N=16 in (13)). Thus, according to (13) and (14), each spline representing one q_i is defined by 18 shaping parameters in the vector X^i. Accordingly, through (15), the total number of optimization parameters amounts to 126.

To conclude, the method described operates so as to meet the following input-output requirements:

Input data

- Initial configuration at takeoff and final configuration at touchdown.
- Amount of angular momentum about the centre of mass (data to be varied from one simulation to another).
- Flight time.

Output

- Time histories of the following variables:
  - Seven angles describing the movement (observed in Koenig's frame).
  - Torque generators at ankles, knees, hips, shoulders, elbows and neck.
- Mechanical energy expended and integral quadratic norm of the mechanical effort produced to generate and control the movement.

The mechanical work done was computed using the time integral of absolute values of joint powers, each one defined as the product of the control torque by the corresponding relative joint velocity.

Results

Numerical simulations were carried out using biometric data of an expert gymnast computed according to De Leva's tables (De Leva, 1996) (Table A1 in Appendix). Limitations of joint movements, as introduced in constraints (11), are specified in Table 1 in accordance with Kurz specifications (Kurz, 1994).

Table 1. Limitations of joint movements

Relative joint rotations	Shoulders θ_4	Elbows θ_5	Neck θ_6	Hips θ_7	Knees θ_8	Ankles θ_9
$\theta_k^{\max}$ (deg)	-5	150	-5	-40	-5	80
$\theta_k^{\min}$ (deg)	-210	5	-20	-180	-130	60

The flight time and the angular momentum at takeoff are basic data featuring the somersault executed. Mean reference values were assessed from selected somersaults performed on stiff floor by a skilled gymnast. They are shown in the first line of data in Table 2. In fact, a more

global data is generally considered as the fundamental characteristic of aerial movements. It is the *rotation potential* defined as the product of the flight time by the angular momentum about the center of mass at takeoff (Yeadon & King, 2002).
The objective of the first three simulations was to compare somersaults resulting from a moderate perturbation of the rotation potential. In Table 2, data for simulations 2 and 3 are deduced from the first one by decreasing the rotation potential $(H \times T = 40)$ to the same value $(H \times T = 35)$. This smaller amount is obtained by reducing the flight time and the angular momentum in the second and third cases, respectively. A further simulation 4 was carried out using an enlarged hip flexion limit while keeping other data of simulation 3 unchanged.

Table 2. Data varied for the simulations carried out

Simulations	Angular momentum H ($kg.m^2.s^{-1}$)	Flight time T (s)	Rotation potential $H \times T$	Hip flexion limit
1	50	0.8	40	-40°
2	50	0.7	35	-40°
3	43.75	0.8	35	-40°
4	43.75	0.8	35	-50°

Stick diagrams of the first three movements generated are displayed in Figure 2. The simulation 1 computed with the reference amount of rotation potential looks like a somersault piked during which legs and arms become almost fully extended.
The next two simulations, computed using the same reduced value of the rotation potential show near identical movements although their respective flight time and angular momentum were noticeably different. They exhibit the same successive piked and tucked phases. At the same percentage of time, the three configurations circled with full lines are tucked in the three cases while the configurations circled with dotted lines are near identical in simulations 2 and 3, these being quite different of their counterpart in simulation 1.

Simulation 4 is set apart in Figure 3 because it results from modifying a different data, the hip flexion limit (see Table 2). As the total body inertia cannot be sufficiently decreased by hip flexion in order to gain enough external rotation velocity, correction is obtained by knee flexion resulting in a tucked configuration throughout the movement.
It is worth noting that the kinematic organization of the first three movements reveals that the effect produced by a modification of the rotation potential $H \times T$ (Table 2) does not show real dependency on one or other of factors H and T. But on the other hand, the minimal cost and the amount of work done are drastically different as shown in Table 3. Particularly, in simulation 2, the mechanical work done has doubled, and the integral amount J of mechanical effort required has increased by 70%.

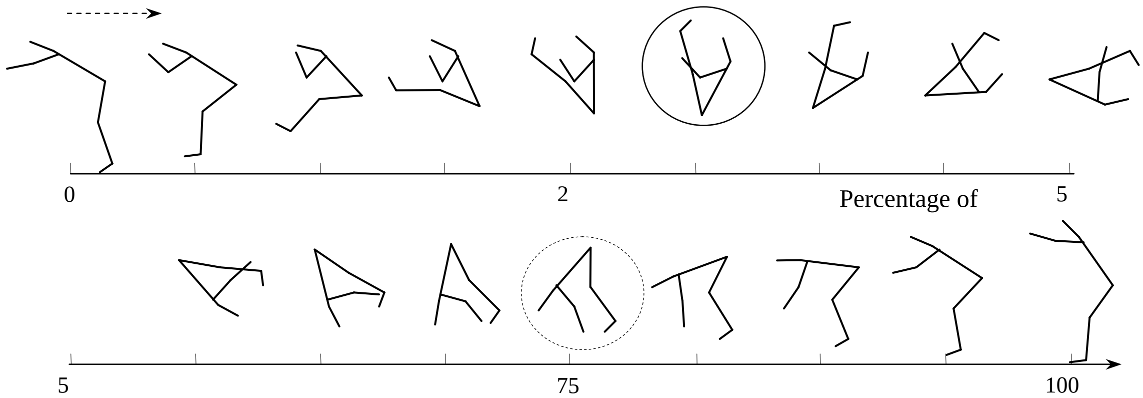

Simulation 1 - Movement generated with the reference value of the rotation potential.

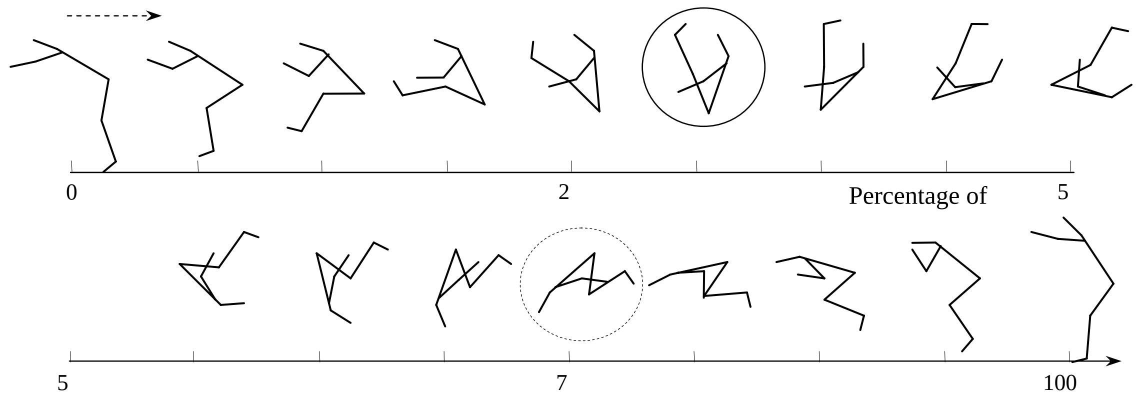

Simulation 2 – Rotation potential reduced by decreasing the movement time

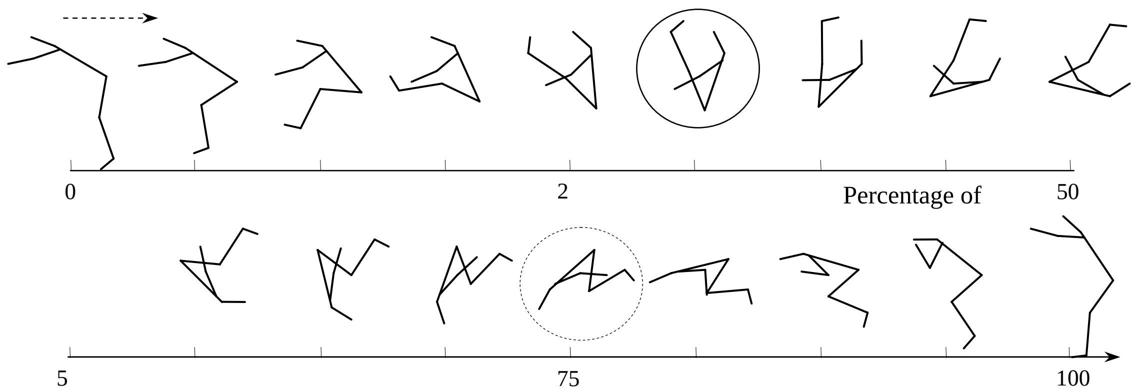

Simulation 3 – Rotation potential reduced by decreasing the angular momentum

Figure 2. *Stick diagrams of the first three simulations*

Time charts of joint torques generated are plotted in Figure 4. Both simulations 2 and 3 produce more variations and greater extremal values of hip and knee actuating torques than the simulation 1. One can also remark that torques in the second case simply amplify, on a shorter time, the variations of their counterparts in the third case.

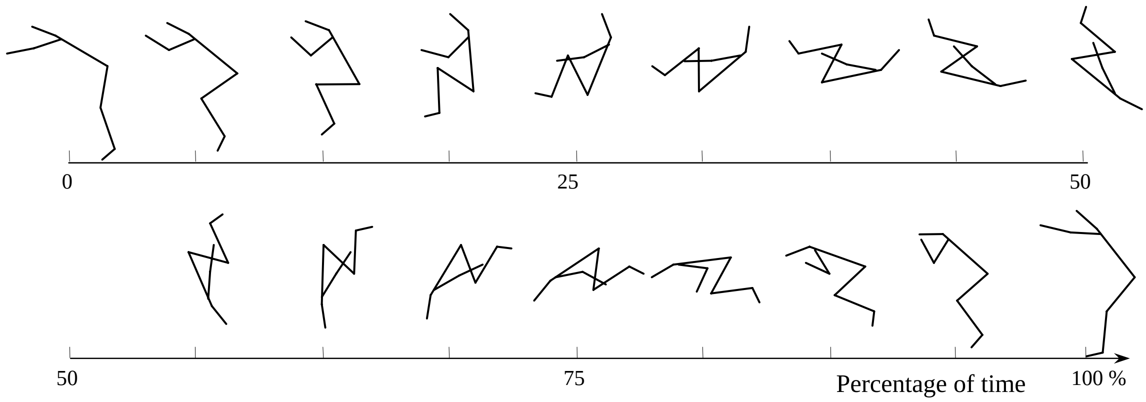

Figure 3. Additional simulation 4

Table 3. Values of minimal cost J and mechanical work done.

Tests	Rotation potential	Hip flexion limit	Minimal cost *J* (dimensionless)	Mechanical work (J)
1	40	-40°	2.64	160
2	35	-40°	4.51	357
3	35	-40°	3.05	269
4	35	-50°	6.69	218

In the extra simulation 4, hip and knee control torques exhibit much less variations than in the above three cases (Figure 5). Actually, they reach and keep simultaneously extremal values during a near steady phase representing about 50% of the movement time. This explains the amounts given in Table 3: the mechanical work is moderate, and even decreased, due to the fact that during the tucked steady phase joint velocities almost vanish, while the actuating effort cost is by far the greatest because the same torques keep their maximal values during the same phase. It must be mentioned that the increase of the minimized criterion is primarily linked to the reduction of the feasible set of the $q_i s$ induced by the slight decrease of the hip flexion range. Also mention that the tucked phase reveals that joint torques match for a while sizeable centrifugal forces, particularly at hip level.

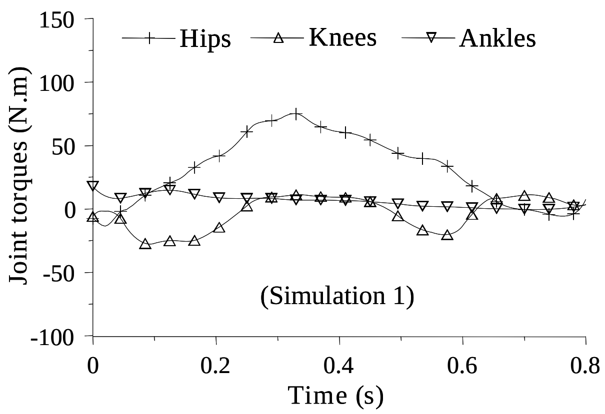

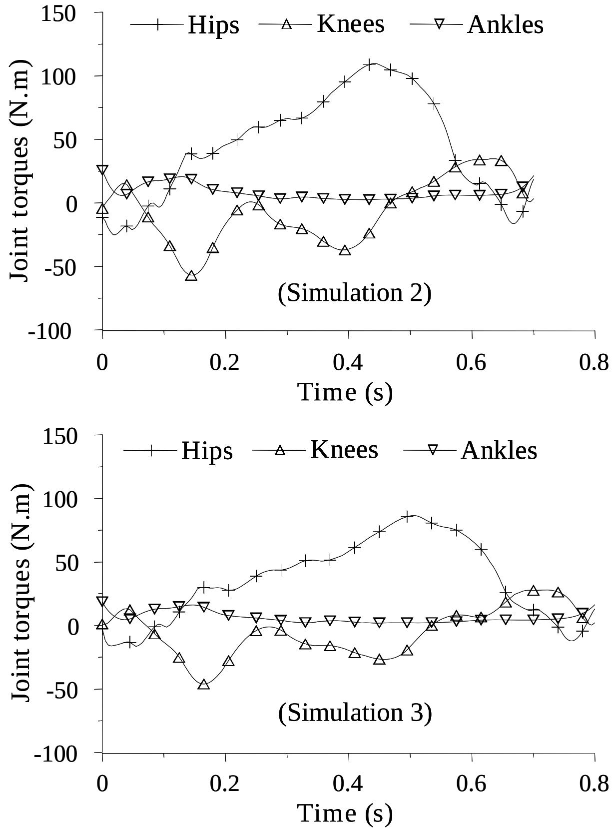

Figure 4. *Simulations 1, 2 and 3: time charts of torque generators at lower limbs.*

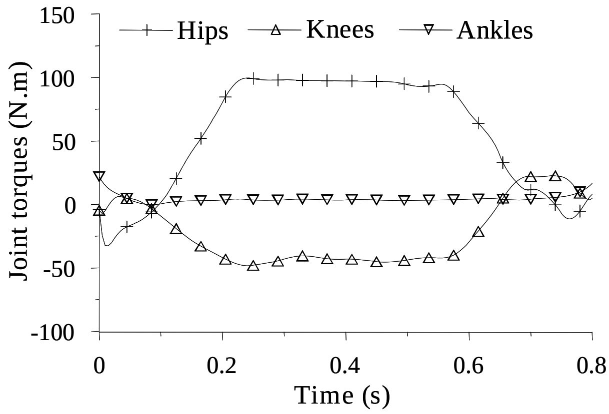

Figure 5. *Simulation 4: time charts of torque generators at lower limbs.*

As an example, Figure 6 shows the time variations of actuating torques generated at shoulders, elbows and neck by the simulation 1. One can notice the relatively high extremal values reached at shoulders, together with the significant values attained at neck. Other simulations exhibit similar values.

Let us recall that in simulation 1, the somersault is piked. In this case, as the legs are in full extension during the grouping, the hip could be considered as a fulcrum about which the two halves of the model rotate. This viewpoint seems to be attested by the sizeable value reached by the torque generator at hips (70 Nm). However, the extremal values of the shoulder torque (40 Nm) show that shoulders provide an essential contribution for the execution of the somersault, and could be seen as a second fulcrum.

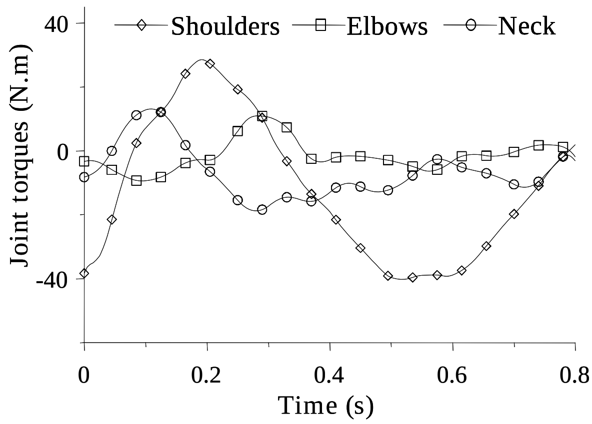

Figure 6. Simulation 1: time charts of torque generators at upper limbs and neck.

Discussion

This paper has shown how a dynamic synthesis method can be used to simulate aerial movements. Non twisting somersaults were generated on the basis of reduced data. The simulations carried out show real similarities with human somersaults piked or tucked. They were focused on the effects produced on the movement by changes of the rotation potential which is a major determinant of the flight phase. It was shown that two movements executed with different angular momenta and flight times, but having the same rotation potential, exhibit the same kinematic organization. The essential difference is a higher price to be paid by the shorter time movement in terms of energy expended and mechanical effort done. Also, it has appeared that a slight change of one physical parameter such as the hip joint rotation limit can produce a major change in the movement organization, and correlatively in the coordination of joint control torques.

Generally, aerial movements are performed with strength and liveliness, and exhibit complex kinematic phases. This makes their experimental analysis using an inverse dynamics approach difficult because movement recording and data processing accumulate experimental uncertainties together with kinematic discrepancies between the recorded movement and its mathematical model, due to numerical processing of raw data, especially when deriving joint and center of mass velocities and accelerations. Although the dynamic synthesis method cannot be substituted for inverse dynamic analysis, it could help to better understand the dynamics of aerial movements by revealing accurately how torque generators match centripetal forces associated with internal rotations and body segment inertia so as to organize the movement in a natural way.

However, this approach raises the question of the relevance of both the performance criterion and the mechanical model used to simulate the movements considered. The criterion implemented in this paper has the ability to generate typical piked and tucked somersaults as performed by gymnasts. Nonetheless, other choices would be possible such as weighted mixed criteria associating the present sthenic criterion with an energetic cost. On the other hand, using two-dimensional models is an approximation. Developing more realistic and multipurpose three-dimensional models is our next objective. Moreover, the aerial phase of a gymnastic exercise depends on the takeoff phase and prepares the touchdown phase. Thus, the final problem to be mastered will consist of dealing with multi-phase movements to be generated as a whole in order to optimize each phase together with the transitions between successive phases.

References

Anderson, F. C. & Pandy, M. G. (2001). Dynamic Optimization of Human Walking. *Journal of Biomechanical Engineering*, 123, 381-390.

Blajer, W. & Czaplicki, A., 2001. Modeling and inverse simulation of somersaults on the trampoline. *Journal of Biomechanics,* 34**,** 1619-1629.

Bobrow, J.E., Martin, B., Sohl, G., Wang, E. C., Park, F. C. & Kim Juggon (2001). Optimal robot motions for physical criteria. *Journal of Robotic Systems*, 18, 785-795.

De Leva, P. (1996). Adjustements to Zatiorsky-Seluyanov's segment inertia parameters. *Journal of Biomechanics,* 29, 1223-1230.

Hull, D. G. (1997). Conversion of Optimal Control Problems into Parameter Optimization Problems. *Journal of Guidance, Control and Dynamics,* 20, 57-60.

Kurz, T. (1994). Stretching Scientifically: a Guide to Flexibility Training, 3rd edition. Stadion Publishing Co.

Leboeuf, F., Bessonnet, G., Seguin, P. & Lacouture P. (2006). Energetic versus sthenic optimality criteria for gymnastic movement synthesis. *Multibody System Dynamics*, 16, 213-236.

Lo, J., Huang, G. & Metaxas, D. (2002). Human motion prediction based on recursive dynamics and optimal control techniques. *Multibody System Dynamics,* 8, 433-458.

Luh, J. Y. S., Walker, M. W. & Paul, R. P. C. (1980). On-Line Computational Scheme for Mechanical Manipulators. *ASME Journal of Dynamic Systems, Measurement and Control*, 102, 69-76.

Pandy, M.G., Anderson, F.C. & Hull, D.G. (1992). A Parameter Optimization Approach for the Optimal Control of Large-Scale Musculoskeletal Systems. *Journal of Biomechanical Engineering*, 114, 450-460.

Requejo, P.S., McNitt-Gray, J.L. & Flashner, H. (2002). An approach for developing an experimentally based model for simulating flight-phase dynamics. *Biological Cybernetics*, 87**,** 289-300.

Ren, L., Howard, D. & Kenney, L. (2006). Computational Models to Synthesize Human Walking. Journal of Bionic Engineering, 3, 127-138.

Seguin P. & Bessonnet, G. (2005). Generating Optimal Walking Cycles Using Spline-Based State-Parameterization. *International Journal of Humanoid Robotics,* 2, 47-80.

Yeadon, M. R. & Mikulcik, E. C. (1996). The control of non twisting somersaults using configurations changes. *Journal of Biomechanics* 29**,** 1341-1348.

Yeadon, M. R. & King, M. A. (2002). Evaluation of a Torque-Driven Simulation Model of Tumbling. *Journal of Applied Biomechanics* 18, 195-206.

Appendix

A1. Biometric data

Table A1. Gymnast biometric data

Segment L_i	Mass (*kg*)	Length (*m*)	Local abscissa of CoG G_i (*m*)	Moment of inertia about G_i ($kg.m^2$)
Feet	2.00	0.16	0.07	0.002
Shins	6.32	0.43	0.19	0.074
Thighs	20.68	0.42	0.17	0.398
Trunk	31.73	0.53	0.29	1.077
Arms	3.96	0.28	0.16	0.022
Fore-arms	2.36	0.27	0.12	0.012
Head	5.07	0.24	0.12	0.042

A2. Backward recursive dynamic model

All movements and formulations are considered in Koenig's frame $(G;\mathbf{X}_0,\mathbf{Y}_0,\mathbf{Z}_0)$.
Further notations defined in accordance with the geometric notations shown in Figure 1:

- $\dot{\theta}_i\mathbf{Z}_0$, rotation velocity vector of body-segment L_i,
- $\mathbf{V}(O_i)$ and $\dot{\mathbf{V}}(O_i)$, $\mathbf{V}(G_i)$ and $\dot{\mathbf{V}}(G_i)$, velocity and acceleration vectors of O_i and G_i, respectively,
- $\mathbf{r}_i = O_iG_i \equiv r_i\mathbf{X}_i$, ($G_i$, center of mass of link L_i),
- $\mathbf{d}_i = O_iO_{i+1} \equiv d_i\mathbf{X}_i,\ i \in \{3,4,7,8\}$; $\mathbf{d}_6 = O_3O_6 \equiv d_6\mathbf{X}_3$,
- $\mathbf{g}$, gravity acceleration vector ($\mathbf{g} = -g\mathbf{Z}_0, g = 9.8\,\text{ms}^{-2}$)
- I_i, moment of inertia of link L_i versus the axis $G_i\mathbf{Z}_0$,
- m_i, mass of link L_i.

For j immediately less than i ($j = i-1$ or $j = 3$):

- $\mathbf{F}_i \equiv \mathbf{F}(L_j \to L_i)$, force exerted by L_j on L_i,
- $\mathbf{M}_i \equiv \mathbf{M}(O_i, L_j \to L_i)$, moment about O_i exerted by L_j on L_i.

A2.1. Kinematic recursion

The hip joint center O_3 was chosen as the starting point for the forward kinematic recursions. First, the velocity of O_3 is derived from the barycentric relationship

$$O_3G = \sum_{i=3}^{9}\mu_iO_3G_i\ ,\quad \mu_i = m_i/(m_3+...+m_9)\,, \qquad \text{(A2.1)}$$

which yields successively

$$\mathbf{V}(O_3) = -\sum_{i=3}^{9}e_i\mathbf{U}_i\ ,\ e_i's \text{ are constant factors and } \mathbf{U}_i = \dot{q}_i\mathbf{Y}_i\,,$$
$$\mathbf{V}(G_3) = \mathbf{V}(O_3) + r_3\mathbf{U}_3\,,$$
$$\dot{\mathbf{V}}(O_3) = -\sum_{i=3}^{9}e_i\dot{\mathbf{U}}_i\ ,\ \dot{\mathbf{U}}_i = \ddot{q}_i\mathbf{Y}_i - \dot{q}_i^2\mathbf{X}_i$$
$$\dot{\mathbf{V}}(G_3) = \dot{\mathbf{V}}(O_3) + r_3\dot{\mathbf{U}}_3\,.$$

Then for $i = 6$, $j = 3$, next for $i = 4{,}5$ and $j = i-1$, and finally for $i = 7$ and $j = 3$, and for $i = 8{,}9$ and $j = i-1$:

$$\mathbf{V}(O_i) = \mathbf{V}(O_j) + d_j\mathbf{U}_j\,,\ \mathbf{V}(G_i) = \mathbf{V}(O_i) + r_i\mathbf{U}_i\,,$$
$$\dot{\mathbf{V}}(O_i) = \dot{\mathbf{V}}(O_j) + d_j\dot{\mathbf{U}}_j\,,\ \dot{\mathbf{V}}(G_i) = \dot{\mathbf{V}}(O_i) + r_i\dot{\mathbf{U}}_i\,.$$

A2.2. Kinetic recursions

Newton-Euler equations are formulated for each link L_i following backward recursions toward the trunk L_3, and initialized at distal links L_5, L_6 and L_9 as follows

$$i \in \{5,6,9\}, \quad \begin{cases} \mathbf{F}_i = m_i \dot{\mathbf{V}}(G_i) \\ \mathbf{M}_i = \mathbf{r}_i \times \mathbf{F}_i + I_i \dot{\theta}_i \mathbf{Z}_0 \end{cases}. \tag{A2.2}$$

Next, one can compute successively

$$i = 4\,;\ i = 8,7\,; \begin{cases} \mathbf{F}_i = \mathbf{F}_{i+1} + m_i \dot{\mathbf{V}}(G_i) \\ \mathbf{M}_i = \mathbf{M}_{i+1} + (\mathbf{d}_i - \mathbf{r}_i) \times \mathbf{F}_{i+1} + \mathbf{r}_i \times \mathbf{F}_i + I_i \dot{\theta}_i \mathbf{Z}_0 \end{cases} \tag{A2.3}$$

Considering that joint dissipative torques are not significant, the six torque generators τ_i are then derived from the six moments computed in (A2.2) and (A2.3) as the trivial dot products $\tau_i = \mathbf{M}_i \cdot \mathbf{Z}_0$ ($4 \le i \le 9$) which result in the set of equation (6) in section 2.2.

It should be noted that above recursions cannot be completed with a final formulation of Newton equation for the trunk L_3. This would lead to a relationship identically satisfied due to the barycentric condition (A2.1). On the other hand, the Euler equation for L_3 together with its six counterparts in (A2.2) and (A2.3) would not be a practical means to derive the condition expressing the conservation of total angular momentum. It is better to formulate directly this condition as indicated below.

A2.3. Angular momentum

The angular momentum H has the same value in both fixed inertial frame and Koenig's frame. It was computed in Koenig's frame using the basic formula

$$H = \sum_{i=3}^{9} \left(I_i \dot{q}_i + \mathbf{Z}_0 \cdot (GG_i \times m\mathbf{V}(G_i)) \right).$$

The Relationship between Ball Speed and Anthropometrical Characteristics among Professional Baseball Pitchers: a Hybrid Evolutionary Algorithm Approach

L. Valandro[1], L. Colombo[1], H. Cao[2], F. Recknagel[2], S. Dun[3], EL. Secco[4]

[1]*Department of Biology, University of Padua, Italy*
[2]*Department of Earth & Environmental Sciences, University of Adelaide, South Australia*
[3]*American Sports Medicine Institute, Birmingham, Alabama*
[4] *Department of Computer Engineering & Systems Science, University of Pavia, Italy*

Abstract

The fastest bowlers and pitchers, who are able to perform at levels that exceed those of their team-mates, should have a combination of optimal physical characteristics and techniques. The relationship between ball speed and anthropometrical characteristics of 48 professional baseball pitchers was investigated using a hybrid evolutionary algorithm (*HEA*). The average height and weight of the subjects were 191.4±4.7 cm and 96.2±8.2 kg, respectively. Their mean brachial index, BI, was 74.9±4.1. Performing our *HEA* analysis led us to discover the best rule sets between different inputs (height, weight, segment lengths) resulting in models relating ball speed to a pseudo-ectomorphic parameter. The robustness of the results was achieved by implementing a parsimonious strategy based on the Akaike criterion as the fitness function. Furthermore, the rule set resulted to be almost always weight greater than constant and after selection of the best pitchers (the lighter ones) the related distribution of speed as a function of BI was shown to be bimodal. These results could be used for talent identification and coaching technique improvement. Our finding could also have some relevance for bio-inspired robotics.

KEY WORDS: ANTHROPOMETRY, BRACHIAL INDEXES, MAXIMUM BALL VELOCITY, GENETIC ALGORITHM, AKAIKE CRITERION, RULE DISCOVERY

Introduction

Fast bowlers and pitchers, who are able to throw the ball faster than their team-mates, should have a combination of optimal physical characteristics and techniques (Carda et al., 1994; Fleisig et al., 1996; Glazier et al., 2000; Valandro et al., 2005). Great values of height and body weight have been reported to be determinants of bowling speed in cricket (Pyne et al., 2005) and throwing sport performance in other sport disciplines (Sidhu et al., 1975; Matsuo et al., 2001).

In this work, we address the problem of predicting ball speed from anthropometric characteristics and the eligibility of rule discovering by a hybrid evolutionary algorithm (HEA). HEA uses genetic programming (GP) to generate and optimize the structure of rule sets and a genetic algorithm (GA) to optimize the parameters of a rule set. Rules discovered by HEA have the IF-THEN-ELSE structure and allow embedding of complex functions in

this work synthesized only from simple arithmetic operators (+, −, *, /). The maximum tree depth and rule set size, together with a parsimonious criterion (Akaike), control the complexity of rule sets (Cao et al., 2006).
From this preliminary work, both talent identification and coaching techniques could benefit as well as biomechanics in general, once other variables (e.g., angles) are included in the rule set discovery. Furthermore, these findings could be of some relevance for bio-inspired robotics.

Materials and Methods

Subjects and Data acquisition

Forty-eight professional baseball pitchers participated in this study. All participants had no previous history of neuro-musculo-skeletal disorders at the time of testing. Prior to the testing, each subject signed a consent form approved by the Institutional Review Board of the American Sports Medicine Institute.
The humeral and radial lengths of each subject's throwing arm were measured prior to biomechanical analysis. The humeral length was measured from the acromion process to the lateral epicondyle and the radial length was measured from the humeral epicondyle to the radial styloid process. The body weight and height were self-reported by each subject (Table 1).

Table 1. Average anthropometric characteristics and age of professional baseball pitchers (mean±SD).

Height *[cm]*	**Weight** *[kg]*	**Arm** *[cm]*	**Forearm** *[cm]*	**Age** *[years]*
191.4 ± 4.7	96.2 ± 8.2	38.73 ± 2.03	28.96 ± 1.54	23.9 ± 3.5

Three different brachial indexes, expressed in terms of length ratios, were compared:

1) The brachial index is defined as:

$$BI = \frac{\text{forearm}}{\text{arm}} \cdot 100$$

2) Another index, derived from *De architectura* by *Marcus Vitruvius Pollio* (27/23 B.C.) and from Leonardo Da Vinci's *Homo Vitruvianus* (1490), is defined as:

$$BI_{L\text{-}V} = \frac{(\text{arm} + \text{forearm} + \text{hand})}{\text{forearm} + \text{hand}}$$

3) An efficacious brachial index is defined as:

$$BI^* = \frac{(\text{forearm} + \text{hand}/2)}{\text{arm}}$$

Hand lengths were derived from allometry.
Before the testing, each pitcher was given ample time for his normal warm-up routine. When the subject was ready, data were collected with the subject pitching off an ATEC (Athletic Training Equipment Company, 18 Santa Cruz, AZ) indoor pitching mound towards a strike zone target located above home plate, 18.4 meters away from the pitching rubber. Each

subject was instructed to pitch ten fastballs with maximal effort. The subject was given 30-60 seconds of rest time before each pitch.
Ball speed was measured in an indoor laboratory with a Jugs radar gun (Jugs Pitching Machine Company, Tualatin, OR) from behind the home plate.

Hybrid Evolutionary Algorithm

HEA has been designed in order to discover predictive rule sets. It firstly evolves the structure of the rule sets by using GP, and secondly optimizes the random parameters in the rule set by using a GA. Rules discovered by *HEA* have the IF-THEN-ELSE structure and allow embedding of complex functions synthesized from various predefined arithmetic operators. The main framework of *HEA* for the rule discovery in the studied data is represented in Figure 1**.** Cao et al. (2006) provided a detailed description of *HEA* including the design of the genetic operators in GP and GA.

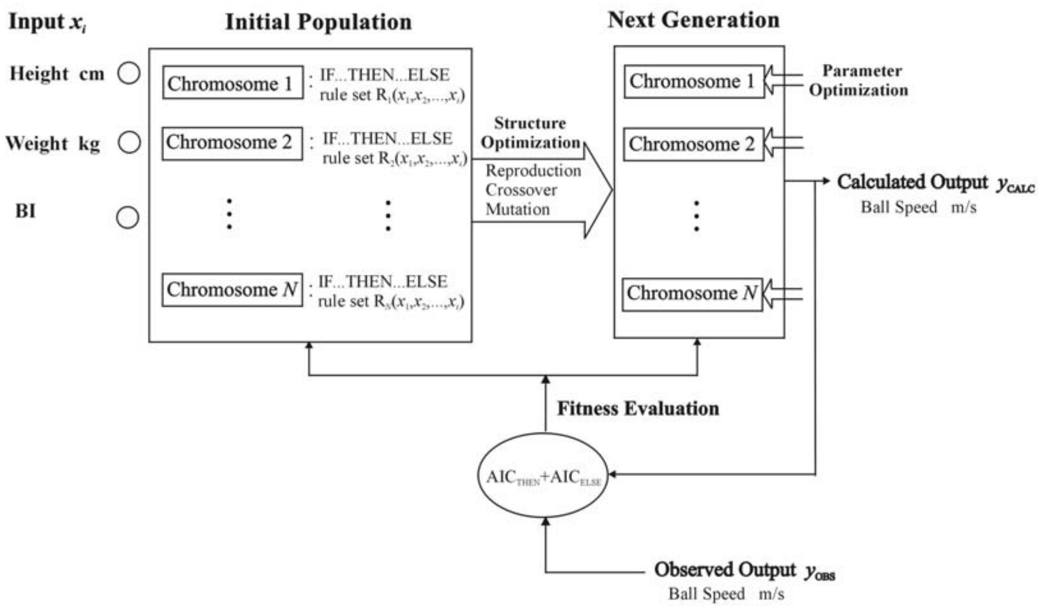

Figure 1. Conceptual diagram of the Hybrid Evolutionary Algorithm for the discovery of predictive rule sets in professional baseball pitchers. The new fitness function keeps into account not only the error but also the number of parameters of the models.

In our analysis, we used the first 24 data points of the measured anthropometric data for training and the remaining 24 data points for testing the generalization behavior of the resulting rule sets. Several analyses of 300 runs were conducted independently. The maximal rule set size was set to be four. All the experiments were performed on a Hydra supercomputer (IBM eServer 1350 Linux) with a peak speed of 1.2 TFlops by using C++ programming language.
The *HEA* was implemented by using anthropometric data as inputs and the measured or observed ball speed (ball $speed_{obs.}$) and the predicted ball speed (ball $speed_{pre.}$) as outputs (Table 2a-b). We started with simple and easily measurable anthropometric variables (Martin et al., 1988).

Table 2a. Input variables used in this study were height, weight, forearm length and arm length (4 inputs). The prediction of ball speed was performed by means of HEA in order to discover rules between variables. Ball speed observed was used to calculate the fitness function.

Height *[m]*	**Weight** *[kg]*	**Forearm length** *[m]*	**Arm length** *[m]*	**Ball Speed$_{obs.}$** *[m/s]*	**Ball Speed$_{pre.}$** *[m/s]*
H_1	W_1	F_1	A_1	s_1	S_1
H_2	W_2	F_2	A_2	s_2	S_2
H_3	W_3	F_3	A_3	s_3	S_3
…	…	…	…	…	…
H_N	w_N	F_N	a_N	s_N	S_N

Table 2b. Input and Output variables (3 inputs) used in the evolutionary modeling of rule sets.

	Variables	**Units**	**Mean±SD**	**Min/Max**
Input variables	X_1 Height	*[m]*	1.914 ± .047	1.80 – 2.01
	X_2 Weight	*[kg]*	96.2 ± 8.2	72.0 – 112.5
	X_3 BI	*[pure number]*	74.9±4.1	65.0 – 86.1
Output variable	Ball speed	*[m/s]*	37.81±1.23	35.32-39.79

The inputs are randomly combined by using the following simple operators +, -, *, / and the best fitting models are selected on the base of number of variables, parameters and error (*see Results*). Figure 2 outlines the flowchart of the detailed algorithm for the rule discovery.

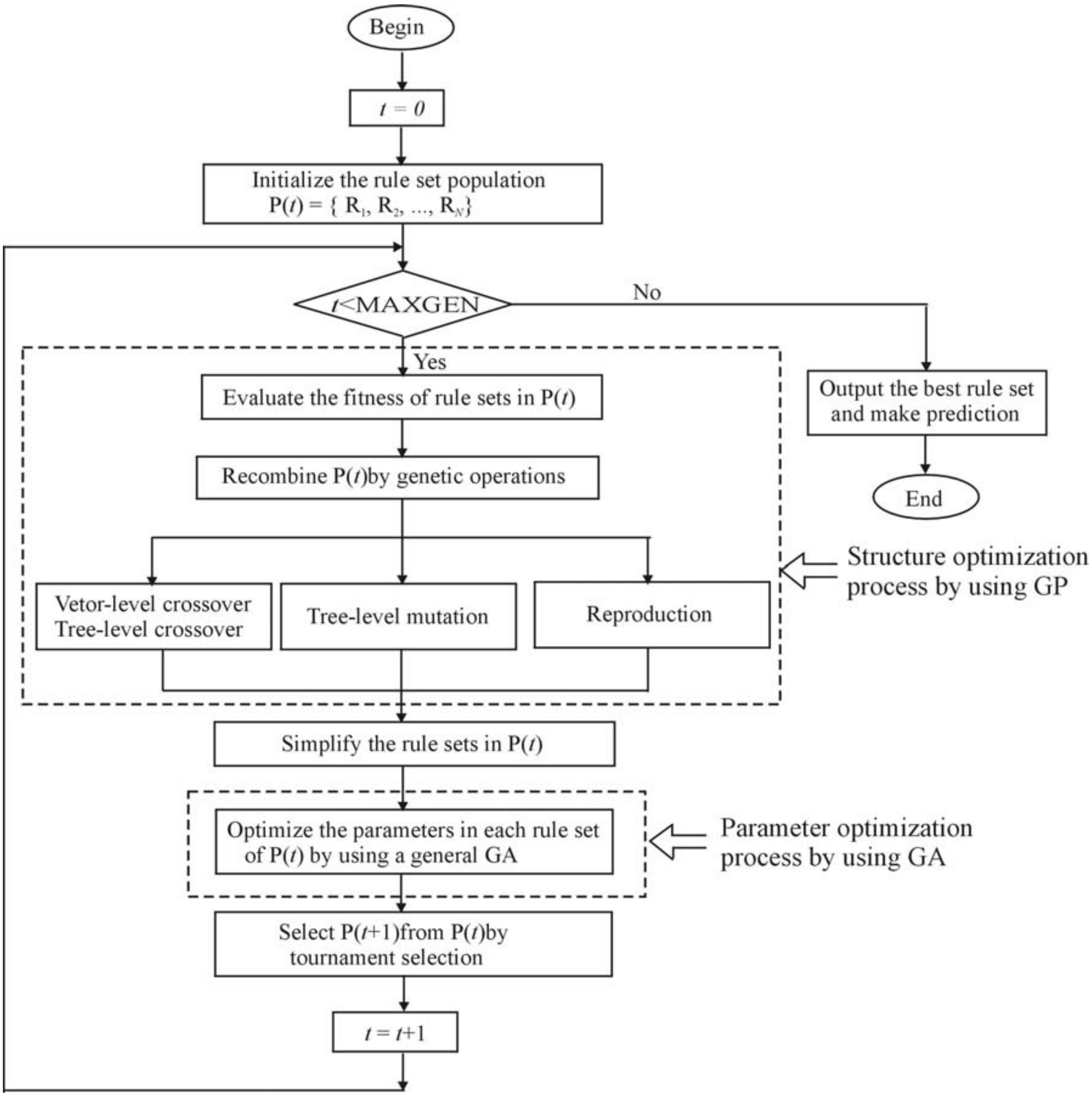

Figure 2 - Flowchart of the Hybrid Evolutionary Algorithm.

Fitness Function

HEA was implemented in C++ by using anthropometric data as inputs and ball $speed_{obs.}$ and ball $speed_{pre.}$ as outputs.

Furthermore, the following corrected Akaike Information Criterion (AIC_c) was introduced in order to reduce overall model complexity (de Leeuw, 1992):

$$AIC_c = AIC + \frac{2k \cdot (k+1)}{(n-k-1)}$$

where *AIC* contains both the error and the number of parameters *k*, while *n* is the sample size. This allowed us to compare pairs of models (THEN and ELSE) derived from each supercomputer run.

The following fitness function was used:

$$\text{AIC} = AIC_{THEN} + AIC_{ELSE}$$

The AIC values used in the fitness function were then compared with other measures of goodness of fit, such as the coefficient of correlation (R) and the Root Mean Square Error (*RMSE*).

Results

The analysis with *HEA* allowed us to identify the most relevant variables to predict both average and maximum ball speeds. Weight was the most selected variable.
Here, we do not present any model including arm length and arm proportions because the solutions of *HEA* were not robust. The comparison of the three BI after analysis with *HEA* showed that the efficacious brachial index was much more frequent than the classical BI and superior to the $BI_{L\text{-}V}$ (see *Materials and Methods*).
Fitting of average and maximum ball speeds with the THEN and ELSE models produced a trivial solution (4 inputs; best AIC):

$$\text{IF weight} < \theta_M$$
$$\text{THEN } S_1, S_3, \ldots, S_N = K_1$$
$$\text{ELSE } S_2, S_6, \ldots, S_{N-1} = K_2$$
$$K_2 < K_1$$

where θ_M is a weight threshold, S_i is the pitcher's ball speed and K_1, K_2 are constants.
After performing 300 more runs (using 3 inputs), three pseudo-ectomorphic models were obtained (Figure 3). Being most subjects fitted by only one of the models (THEN and ELSE), the rule discovery tool becomes an equation discovery one (Table 3).

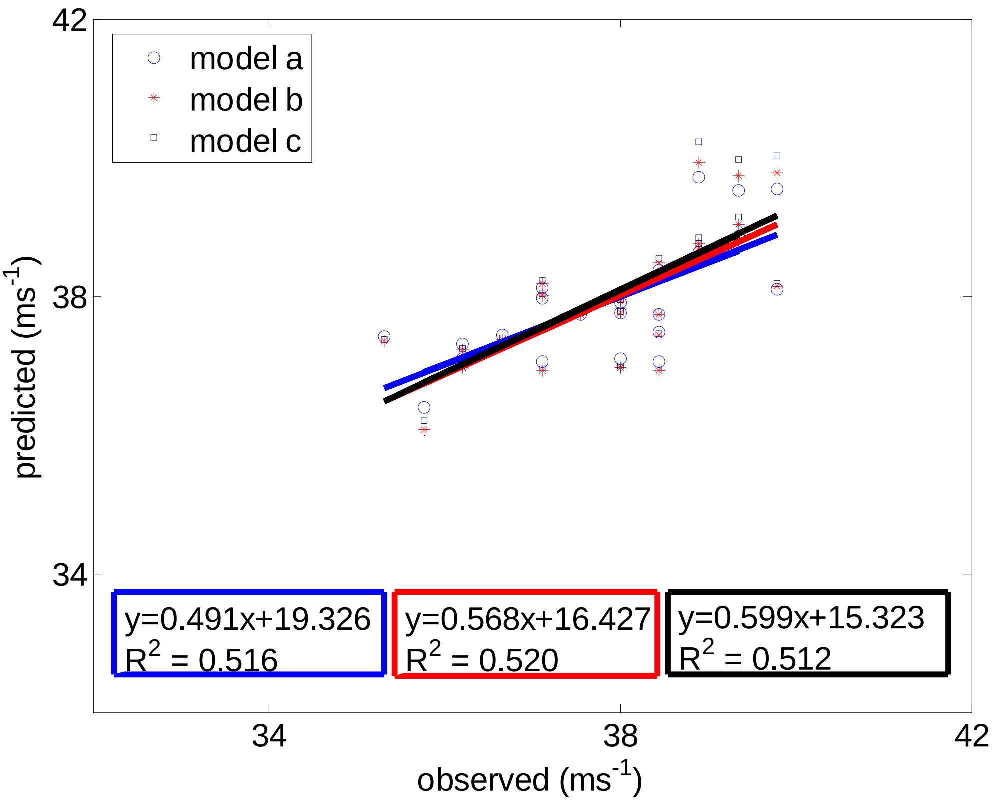

Figure 3. R^2-values for linear correlation between ball speed observed and predicted by model with best AIC (model a), 8th best AIC (model b) and 3rd best AIC (model c) (training data, N=23).

Table 3. Best ectomorphic models fitting the data. F (x) is ball speed (mph), x1 is height (cm) and x2 represents weight (kg).

F(x)=(x1/(x2+x2+x1))*167.886	**best AIC**	**1 const**	**(a)**
F(x)=(133.799-(x2*99.899)/x1))	**8th best AIC**	**2 consts**	**(b)**
F(x)=((24.794*(x1/x2))+34.313))	**3rd best AIC**	**2 consts**	**(c)**

The testing has been extended to the remaining unseen data (data not seen from the algorithm) (N=17) for all three models (Figure 4a). Seven subjects with extreme body mass index (BMI) values, were excluded as outliers.

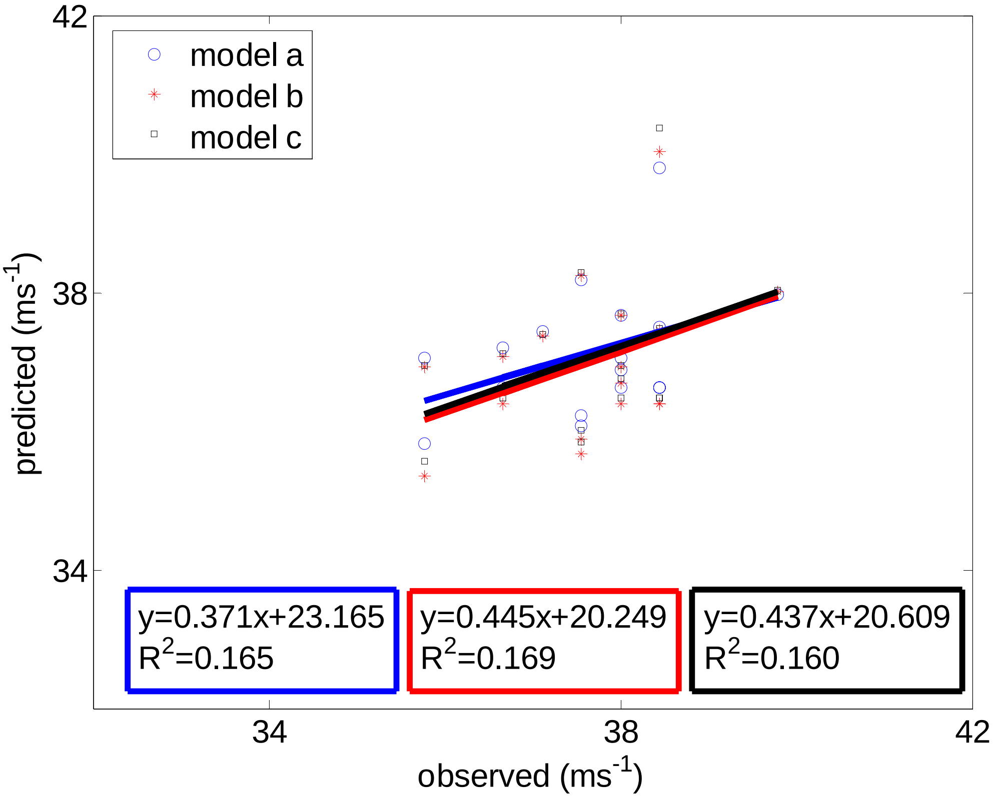

Figure 4a. R2-values for linear correlation between ball speed observed and predicted for the three pseudo-ectomorphic models (unseen testing data, N = 17).

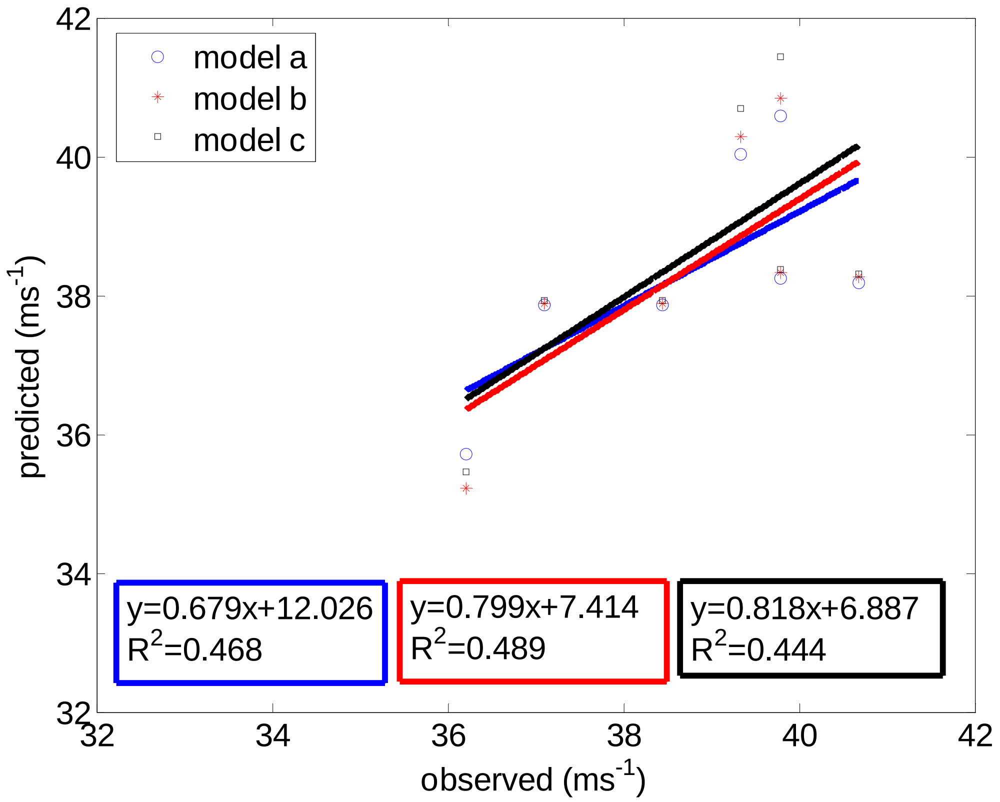

Figure 4b. R2-values for linear correlation between ball speed observed and predicted for the three pseudo-ectomorphic models (unseen testing data, N = 7).

Table 4a. Coefficient of correlation, R, for observed versus predicted ball speed (data not fitted by most models in previous runs and for which the difference between ball speed observed and predicted was greater than 2,5 m/s were considered outliers).

	Training Data (N=23)		
Model	**a**	**B**	**c**
R	0,718	0,721	0,715
	Testing Data (N=17)		
Model	**a**	**B**	**c**
R	0,401	0,411	0,400

A further testing of the generalization behavior of the three models has been performed on 10 professional baseball pitchers whose data were collected with the same protocol (Figure 4b). Again 30% of the athletes were excluded from the analysis following the same criteria.

Table 4b. Coefficient of correlation, R, for observed versus predicted ball speed (data for which the difference between ball speed observed and predicted was greater than 2,5 m/s were considered outliers).

	Testing Data (N=7)		
Model	**a**	**B**	**c**
R	0,684	0,699	0,666

The maximum ball speed predicted by the three models (weight 72 *kg*; height 183 *cm*) is always less than 100 *mph*, the model c being the closest (97.32 *mph* = 43.51 *m/s* = 156.64 *km/h*). Model b improves the coefficient of correlation in both the testing procedures, both in the remaining athletes (N=17) as well as in the post-hoc collected ones (N=7).

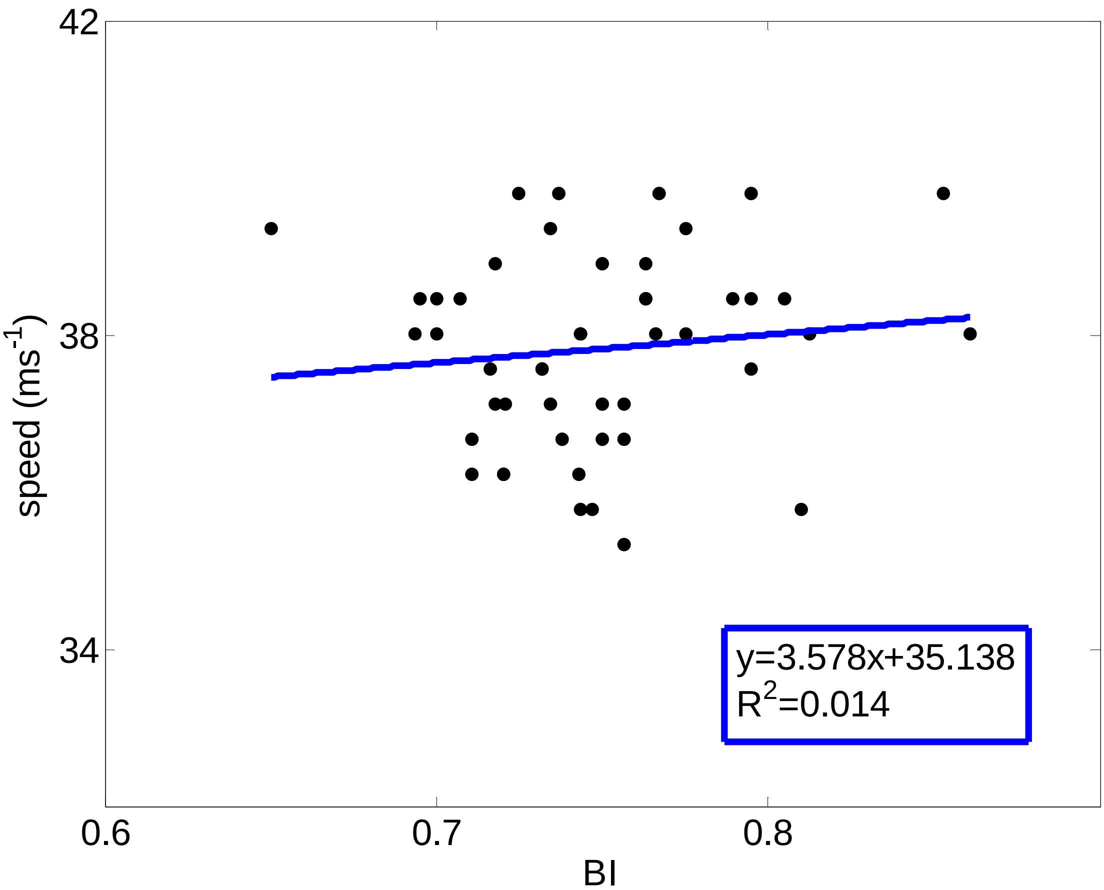

Figure 5. Ball speed as a function of BI (N = 48; p = 0.89).

Bimodality of Ball Speed as a Function of BI

The correlation of BI with ball speed (Figure 5) was not significant (p = 0.89), while after selection of lighter subjects throwing faster, a bimodal distribution of speed appeared, but the linear correlation was still obviously not significant (p = 0.98) (Figure 6).

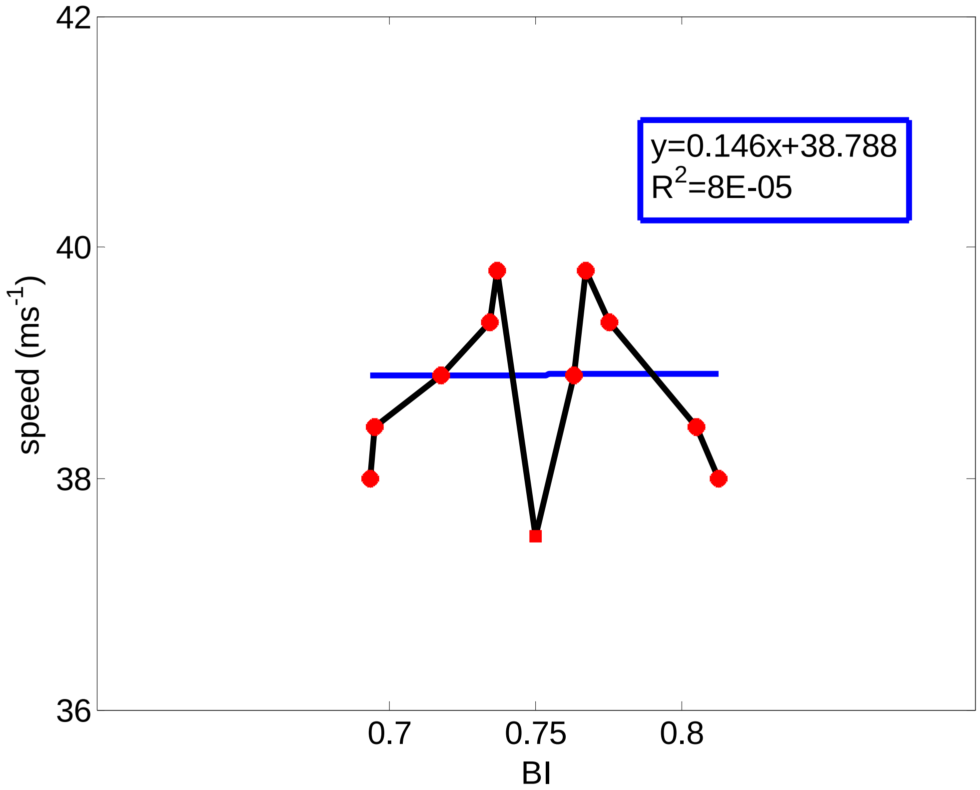

Figure 6. Ball speed as a function of BI after selection of pitchers with weight less than 92 kg (N = 10; p = 0.98).

Discussion

Increases in height and weight have been observed and associated in elite baseball athletes to improved performance (Silver, 2005: see http://www.baseballprospectus.com/article.php?articleid=3979).

In this study, high values of height and inversely small values of body weight were reported to be determinants of throwing sport performance contrarily to Pyne et al (2005) for cricket. His finding could be reconciled with our data considering a parabolic function of ball speed as a function of body weight.

Since the ectomorphic model derived from baseball pitchers was also used for predicting speed in fast-medium bowlers using anthropometric data from Glazier et al. (2000) (*in preparation*), we propose that, although Pyne and co-authors' work has relevant practical implications, it could be misleading when indicating weight as a main variable in the senior-junior comparison. Matsuo et al. (2001) found that a faster throwing group of pitchers was significantly taller than the slower throwing group. In addition, subjects in the taller group have longer arms, as discussed by Garda et al. (1994). According to their somatotype analysis, future work should investigate not only the relevance of weight, but also the distribution of masses for speed prediction.

Analyzing an exiguous sample of front-on fast-medium bowlers, subjects displaying more ectomorphic characteristics were faster (Valandro et al, 2005). In this work, the *HEA* discovered simple models with good prediction power. Although Matsuo et al. (2001) found a non-significant difference between the weights of faster and slower groups, in our work weight was the most commonly selected parameter to derive the two sets of points to be fitted

with the THEN and ELSE models. *HEA* offered a rough simplistic solution, although not highlighting any relevant variables, where the fitting of pitchers' speed was possible with merely a constant K_1 = 83.79 for the heavier group and a constant K_2 = 87.39 for the lighter group. It nicely explains how the lighter athletes were able to throw faster (THEN MODEL) than those athletes weighing above a certain threshold (θ_M = 92 *kg*) (ELSE MODEL).
The model (a) with the best AIC was reported here because it could fit the data with only one constant. However the most reliable model is the pseudo-ectomorphic one (b), which allows the estimation of the maximum ball speed theoretically possible and improves the error after generalization to all professional pitchers (8^{th} best AIC). The maximum ball speed predicted using a formula containing only height and weight variables was 94.49 *mph* = 42.25 *m/s* = 152.09 *km/h*, in any case less than 100 *mph* even when using the lightest subject (72 *kg*; 183 *cm*).
The three models presented were not able to predict all points, leaving space to biomechanical interpretation (*e.g.*, Fleisig et al., 1996). It should be noted, however, that the subjects not fitted by the three models were consistently the same, indicating the robustness of the method. Indeed, the introduction of the corrected AIC_c, that takes into account the small sample size, led us to select the most parsimonious models increasing the robustness of *HEA* (Akaike, 1973; Sugiura, 1978; see also de Leeuw, 1992 for a review). AIC trends were almost always comparable to those of coefficient of correlation and other error functions, meaning that each run with good AIC was associated with small error functions.
The *HEA* approach is an adaptive method, which mimics processes of biological evolution, genetic variation and natural selection and searches for suitable representations of a problem solution by means of genetic operators and the principle of survival of the fittest (see Holland, 1975; Goldberg, 1989; Valandro et al., 2000; Cao et al, 2006). It seems very promising and will soon be applied in the discovery of a more refined and general model and in the evaluation and guide of coaching techniques.
Here, we did not consider models containing arm length and body proportions because *HEA* results were not robust. However, the analysis with *HEA* showed that the efficacious brachial index was much more frequent than the classical BI and superior even to the BI_{L-V} index.
The possibility of a bimodal distribution of speed as a function of BI after selecting a sub-sample as indicated by the *HEA* (Rule set, weight<w_x) is of great interest and could be explained by the minimum jerk theory (Secco et al., 2005). The greater usability, *i.e.* the amount of all the admissible reachable positions (Caimmi et al, 2005) of the subjects with BI* = 1, could imply a less efficient movement control by the brain which in turn would yield smaller ball velocity with respect to a slightly lower usability but with more efficient movement control and then higher ball velocity. This bimodal finding was also observed in the frequency of brachial indexes of Olympic rowing athletes, both males and females, indicating that this is possibly quite a general phenomenon (Valandro et al., *unpublished*).
Future work will try to interpret such kinanthropometric result (bimodality) by means of biomechanical analysis (Bartlett et al., 1996; Escamilla et al., 2001).

Acknowledgements. We would like to acknowledge Prof. Giovanni Magenes and Benedetto Salvato for discussion and for supervising this work. Thanks to Francesca De Conti for carefully reading through the manuscript. Thanks to Dr. Roberto Caimmi for helpful discussion and careful reading through the manuscript. Last, but not least we would like to acknowledge Dr. Glenn Fleisig, the Director of the American Sport Medicine Institute for providing the data and for helpful discussion.

References

Akaike, H., (1973). Information Theory as an Extension of the Maximum Likelihood Principle. In Petrov, B.N. & Csaki, F., *Second International Symposium on Information Theory*, *Akademiai Kiado*, Budapest, 267-281.

Bartlett, R.M., Stockill, N.P., Elliot, B.C. & Burnett, A.F. (1996). The Biomechanics of Fast Bowling in Men's Cricket: a Review. *Journal of Sports Sciences, 14*, 403-424.

Caimmi, R., Secco, E.L., Valandro, L., Magenes, G. & Salvato. B. (2005). Potenza Cinematica dell'Arto Superiore: Modello a Minimo Jerk. In *BIOSYS 2005 (Anipla), Sistemi di Ingegneria Biomedica*, 81-95.

Cao, H., Recknagel, F., Kim, B. & Takamura, N. (2006). Hybrid Evolutionary Algorithm for Rule Set Discovery in Time-Series Data to Forecast and Explain Algal Population Dynamics in Two Lakes Different in Morphometry and Eutrophication. In: *Ecological Informatics. Friedrich Recknagel.* (2nd Edition) Springer-Verlag Berlin, Heidelberg, New York, *17*, 347-367.

Carda, R.D. & Looney, M.A. (1994). Differences in Physical Characteristics in Collegiate Baseball Players. *Journal of Sports Medicine and Physical Fitness, 34*, 370-376.

de Leeuw, J. (1992). Introduction to Akaike (1973) Information Theory and an Extension of the Maximum Likelihood Principle. In: Kotz, S. & Johnson, N. L. (Eds.), *Breakthroughs in statistics, Vol. 1*. Springer-Verlag, London, 599-609.

Escamilla, R.F., Fleisig, G.S., Zheng, N., Barrentine, S.W., Andrews, J.R. (2001). Kinematic Comparisons of 1996 Olympic Baseball Pitchers. *Journal of Sports Sciences* 19: 665-76.

Fleisig, G.S., Barrentine, S.W., Escamilla, R.F. & Andrews, J.R. (1996). Biomechanics of Overhand Throwing with Implications for Injuries. *Sports Medicine*, *21*, 421-437.

Glazier, P.S., Paradisis, G.P. & Cooper, S-M. (2000). Anthropometric and Kinematic Influences on Release Speed in Men's Fast-Medium Bowling. *Journal of Sports Sciences*, *18*, 1013-1021.

Goldberg, D.E. (1989). Genetic Algorithms in Search Optimization, and Machine Learning. *Addison-Wesley*, New York.

Holland, J. (1975). Adaptation in Natural and Artificial Systems. *The University of Michigan Press*, Ann Arbor.

Martin, A.D., Carter, J.E., Hendy, K.C. & Malina, R.M. (1988). Segment Lengths. In: Lohmann, T.G., Roche, A.F., & Martorell, R. (Eds.). *Anthropometric Standardization Reference Manual*, Champaign, IL, Human Kinetics, 9-26.

Matsuo, T., Escamilla, R.F., Fleisig, G.S., Barrentine, S.W. & Andrews, J.R. (2001). Comparison of Kinematic and Temporal Parameters between Different Pitch Velocity Group. *Journal of Applied Biomechanics*, *17*, 1-13.

Pyne, D.B., Duthie, G.M., Saunders, P.U., Petersen, C.A. & Portus, M. (2006). Anthropometric and Strength correlates of Fast Bowling Speed in Junior and Senior Cricketers. *Journal of Strength and Conditioning Research*, *20*, 620-626.

Secco, E.L., Valandro, L., Caimmi, R., Magenes, G., Salvato, B. (2005). Optimization of Two-joint Arm Movement: a Model Technique or a Result of Natural Selection? *Biological Cybernetics*, *93*, 288-306.

Silver, N. (2005). Lies, damned lies. Does size matter? In: http://www.baseballprospectus.com/article.php?articleid=3979

Sidhu, L.S., Kansal, D.K., Kanda, B.S. (1975). Anthropometric and Roentgenogrammetric Assessment of Physique and Body Composition of Athletes Specializing in Throwing Events. *Journal of Sports Medicine*, *15*, 192-198.

Sugiura, N. (1978). Further Analysis of the Data by Akaike's Information Criterion and the Finite Corrections. *Communications in Statistics*, Theory and Methods A7, 13-26.

Valandro, L., Salvato, B., Caimmi, R. & Galzigna, L. (2000). Isomorphism of Quasispecies and Percolation Models. *Journal of Theoretical Biology, 202*, 187-194.

Valandro, L., Caimmi, R., Drusini, A., Glazier, P., Henneberg, M., Salvato, B. & Secco, E.L. (2005). Kinanthropometry and Biomechanics applied to Talent Identification of Bowlers in Cricket. 9th International Scientific Conference. In: *Human Kinetics, IASK 2005*, Rimini, Italy.

„sail:lab" - A novel Package for Sailing Simulation, Scientific Visualization and E-Learning

F. Bünger[1], S. Busch[2], I. Gasser[1], S. Günzel[1], A. Hebbel-Seeger[2], M. Mohr[1]

Hamburg University, Department of Mathematics[1] & Sport Science[2]

Abstract

"sail:lab", as an interdisciplinary project of mathematicians and sport scientists, uses the physical description of sailing to develop an E-Learning component, which can be integrated in Blended Learning scenarios in both departments. By calculating the forces and moments due to wind and current which act on sail, hull, rudder, and fin, the movement of a jolly-boat is visualized. A real time computation and a graphical user interface, which accomplishes the association of sailing instruments, enable an intuitive use, especially for sailing experienced users. So, "sail:lab" provides a theory - practise transfer, offering the possibility of a deeper understanding of sailing physics for sport students. In the opposite this simulation process is a good example for practise – theory transfer in mathematics.

KEY WORDS: SIMULATION, SAILING, DIFFERENTIAL EQUATIONS, CONTEXT-SENSITIVE USE

Introduction

Simulations fulfil many purposes. By modelling and simplifying reality, causal coherence becomes obvious. This refers to both the parameters of the underlying model and the variables of the simulated domain. Theses positive effect are described by Perl, Lames and Glitsch (2002, p. 31). But the authors warn that simulations which are technically too complex may draw the user's attention away from true nature of the system being simulated

The hereby presented project "sail:lab" is based on the these ideas of causal coherences. It is an interdisciplinary development of the department of mathematics and the department of sport sciences at the University of Hamburg. In the first instance the object of this joint venture is to develop a physical-mathematical model for the simulation of a moving sailing boat. The pursued result of a stand-alone application should then enrich the teachings of both departments. On the one hand within mathematics it can be used as an ideal type possibility of modelling with differential equations (the underlying models are based on differential equations). On the other hand in the context of sport studies, a quantitative simulation like this, provides an improved transfer from theory to practical experience in the field of sailing education.

The development of learning objects in sport science for different user-groups is also described by Kibele (2005): The simulation proposed by Kibele is based on the net-working of sport science, physics and school user-groups. The primary object of Kibele's Simulation is however the gaining of knowledge in the field of sport-science, more exactly, in bio-mechanics. In contrast to this, the simulation presented here should provide information which may be differently interpreted by the user-groups involved. As an example; the use of

differential calculus is of interest to the mathematicians, the sport-scientists will be interested in the visualisation of the magnitude and effect of the different influences upon a sailing boot. Perl, Lames and Glitsch (2002, p. 31) draw a distinction between simulation and animation, technical developments in recent times are however gradually blurring the borders between these concepts. According to Perl, Lames and Glitsch a simulation is “the prediction of (a movement) taking into account the laws of mechanics, the forces acting on the system and the prevailing conditions.” Whereas animation is “the dynamic representation of model-data and calculations” (Perl, Lames & Glitsch, 2002 p.126). Within the frame-work of this article, when the simulation “sail lab” is referred to, we mean both simulation of movement and animation.
In the presented contribution we will outline the technical-mathematical side of the project first, followed by considerations of the interdisciplinary deployment scenarios from a didactic-methodical point of view.

Modelling

We postulate the physical dimension of the boat to be given. After definition of different input data - like a two dimensional wind field, a two dimensional current field, the position of sail and aviation and the position of the sailor on the boat (modifiable during calculation process) – the user receives the output data relevant for the sailor: The position of the sailing-boat, the components of the velocity, the angle of direction and the angle of velocity, the heel and the rate of change of the heel angle. The corresponding balance equations of dynamical forces yield a system of differential equations, calculated in a real-time operation.
The main part of the mathematical model consists in the calculation of the forces F, which drives the boat into motion, and the numerical solution of the kinetic equation of motion. All values will be considered in two coordinate systems, one fixed system (x,y,z) and another one (ξ,η,ς) moving with the boat, as shown in figure 1.

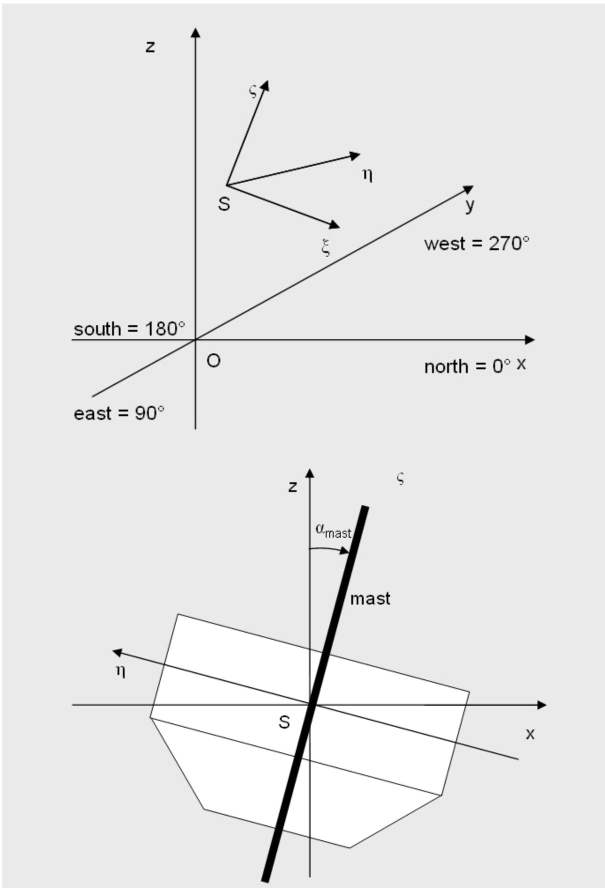

Figure 13: Coordinate Systems - fixed System (x,y,z) and boat system (ξ,η,ς).

Decisive for the movement of the boat are the forces due to wind (sail-force) and due to current (hull-force).
Atmospheric wind and fair wind are accumulated up to the apparent wind. The sail force can be divided into two components, the buoyant force A_{sail} vertical and the resistance force W_{sail}

parallel to the direction of apparent wind, pictured in figure 2. Buoyant and resistance coefficient C_A respectively C_W, depend on the angle between wind direction and sail and can be taken from tables, which are part of the program. So buoyant force and resistance force can be calculated due to

$$A_{saill} = \frac{1}{2} C_A \cdot s \cdot v_\infty^2 \frac{p}{RT}$$

$$W_{sail} = \frac{1}{2} C_W \cdot s \cdot v_\infty^2 \frac{p}{RT}$$

where s is the surface area of the sail and v_∞ is the velocity of the apparent wind. The density of wind current is air pressure p divided by air temperature T and universal gas constant R.

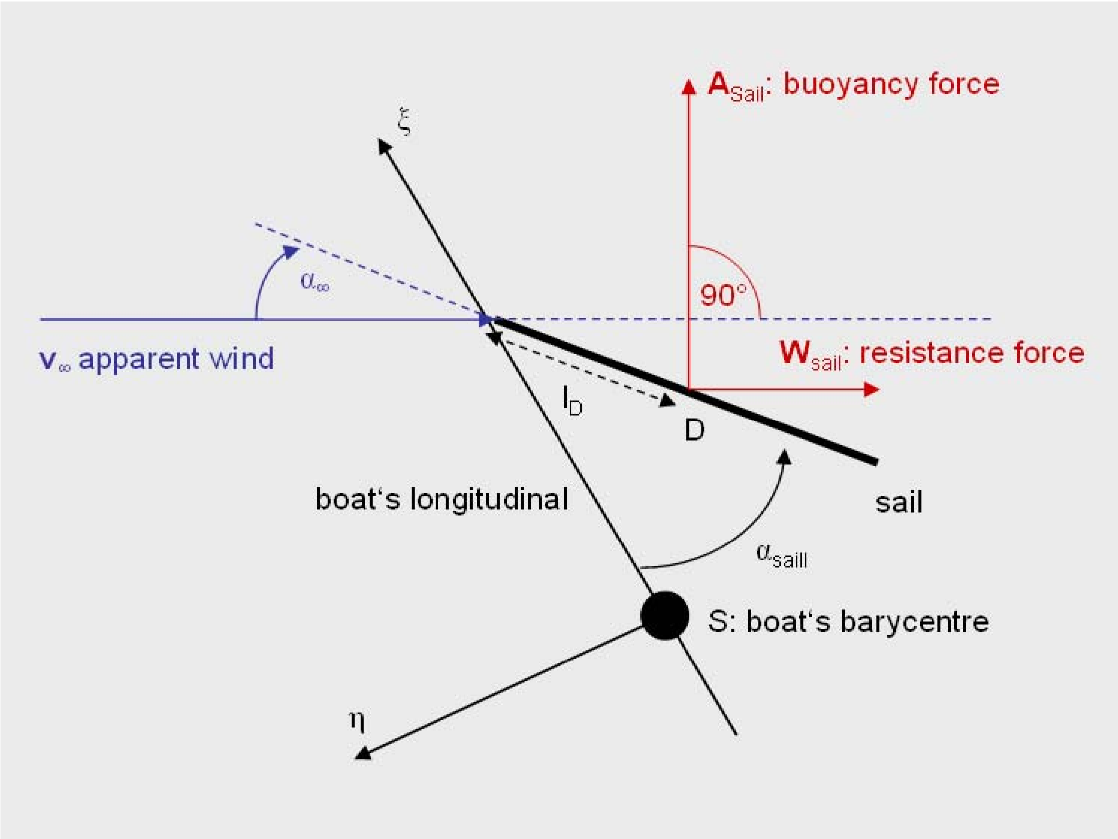

Figure 14: The sail force can be divided into two components, buoyant force A_{sail} and resistance force W_{sail}.

The torsional moment is related to the ζ-axis (the attitude axis) due to the sail and therefore is given by the cross product of the sail force and the position vector of sail pressure point.
The subaqueous hull force is generated by the current. Analogue to the wind the apparent current v_{ocean} is the summation of ocean current and fair current. The force to the hull is dynamical pressure multiplied by area of hull surface. Thereby the dynamical pressure p is given due to

$$p = \frac{1}{2} \rho \cdot v_{ocean}^2$$

with the density of water named ρ.
The hull by itself can be approximated by the use of a cylinder with a polygonal base area and constant height. For each base area (i is the number of polygonal sides) the force can be calculated as

$$F_i = p \cdot A_i = \frac{1}{2} \rho \cdot A_i \cdot v_{ocean}^2 .$$

where just the normal components v_{in} take effect to the product. The hull force is the sum of these forces and takes effect at the lateral pressure point (LDP), which is assumed to be in the middle of the fin, see figure 3 for explanation. Equally the torsional hull moment (concerning the ζ-axis) results from the summation of torsional hull moments at the different polygon boat sides.

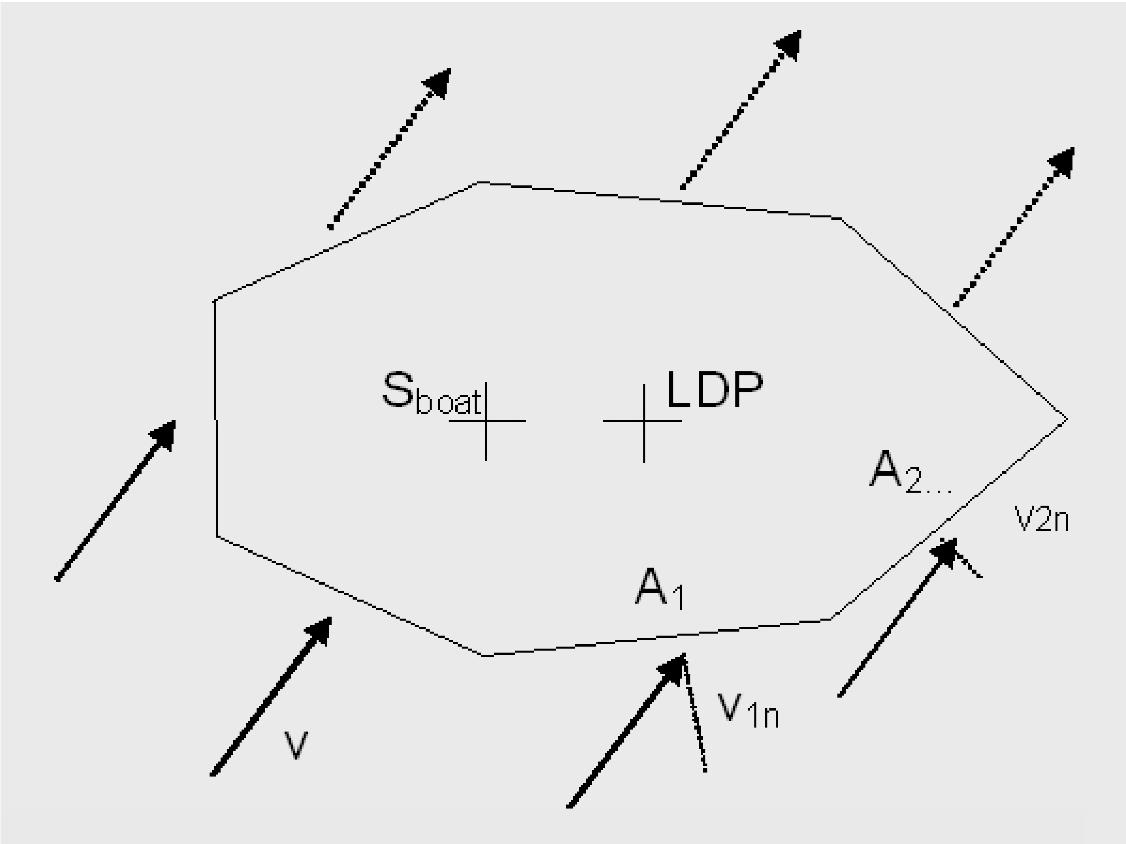

Figure 15: The hull is approximated by a cylinder with polygonal base area. The current yields a printing pressure normal to the endwalls, while the traction force can be neglected.

Further forces yield the impact due to the apparent current along fin and rudder. Both are conceived as flat planes in the water. The incident flow induces buoyant and resistance force, where the vertical component of force can be neglected. As pressure point we choose the plane center so the resulting moment (regarding the ζ-axis) at the barycentre of the boat can be calculated concerning the position of these midpoints.
The heel of the jolly-boat originates in the moment of sail and fin in respect of the axis of gyration, which is assumed to be the longitudinal ξ-axis, see figure 4 for details. So the barycentre is part of the axis of rotation. The uplifting moment of the boat and the sailor act in opposition to the sail- and fin moment. If I is defined as the moment of inertia accumulating boat and sailor and α is the angle of heel we get the equation

$$I\ddot{\alpha} = M_{sail} + M_{helmsman} + M_{fin} + M_{up}$$

where M_i is the respective moment concerning the ξ-axis and the uplifting moment M_{up} depends on the angle of heel and can be taken from a boat specific table.

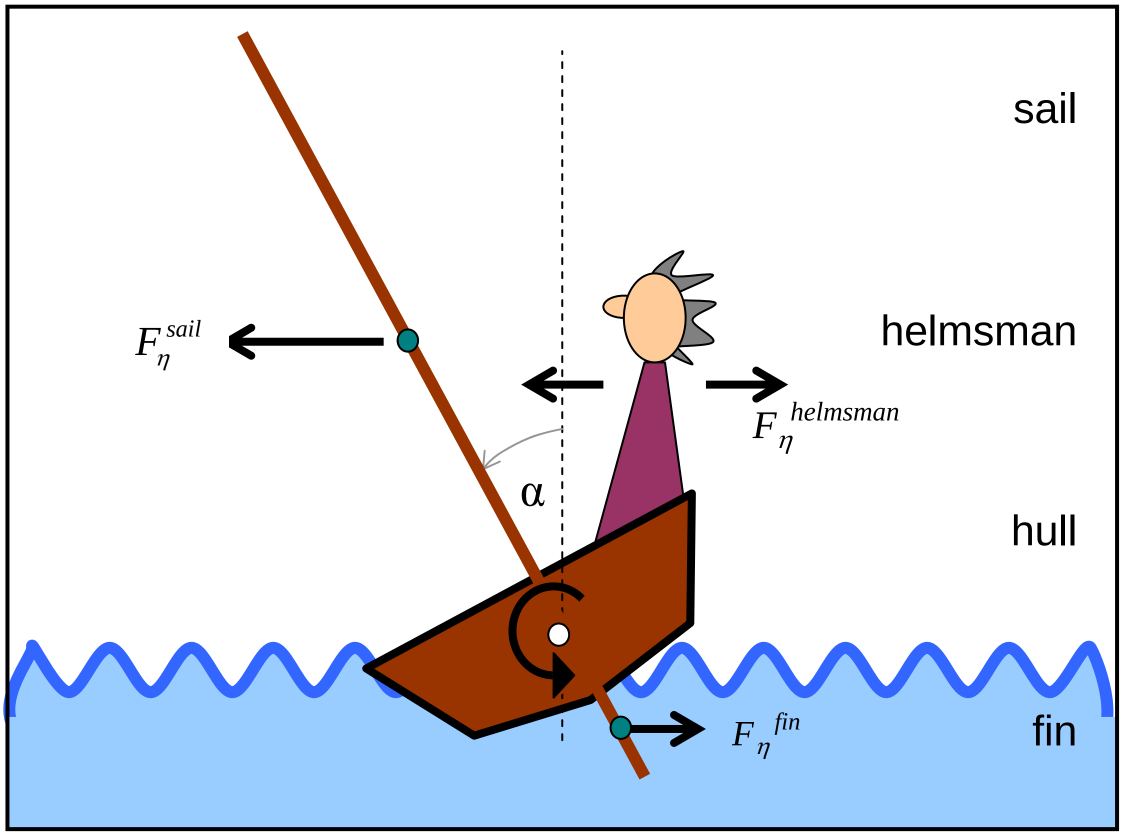

Figure 16: The heeling is forced by the sail force and the force onto the fin, the position of the sailor and the uplifting moment operates contrarily.

The equation of motion therefore appears as a system of eight differential equations, which should be computed numerically:

$$\dot{x} = u$$
$$\dot{y} = v$$
$$\dot{u} = \frac{1}{m} F_x$$
$$\dot{v} = \frac{1}{m} F_y$$
$$\dot{\varphi} = v_\varphi$$
$$\dot{v}_\varphi = \frac{M_\varsigma}{I}$$
$$\dot{\alpha} = v_\alpha$$
$$\dot{v}_\alpha = \frac{M_\xi}{I}$$

where the following terms were used:

- x and y are absolute coordinates referring to the fixed system
- u and v are velocities in x, y direction
- φ is the horizontal angle of the boat
- v_φ is the velocity of rotation
- α and v_α are the vertical rotation angle respectively the longitudinal axis of the boat and the time rate of change
- M_ζ and M_ξ are the resulting moments of the boat concerning to the ζ-axis (horizontal rotation) and ξ-axis (vertical rotation).

The solution is determined with the help of the procedure of Runge and Kutta as it is applied by Dormand and Prince with the order of p=5, q=4 (cp. Dormand & Prince, 1980; Papacostas & Papageorgiou, 1996), known in MATLAB as ode45. For a better performance we use a minimal increment.
At the end all relevant parameters are placed to the users' disposal: position, course, velocity, heel, position of fin and sail with respect on the axis, magnitude and angle of apparent wind and apparent current, position of the sailor.

Realisation

The model was implemented in the Macromedia Tool Director MX 2004. The aim was to design an interactive tool such that the user can interfere continuously by changing appropriate parameters. The mentioned Macromedia tool is based on the object oriented program language Lingo. As an important requirement we postulate that "sail:lab" can be both distributed as individual application and used via Internet as Shockwave-Plug-in.
The graphical design is similar to the Flash-based sailing-software „e-törn" (Hebbel-Seeger, 2003). However, the underlying concept is fundamentally different. „e-törn" reduces the system boat – sailor to a few basic relations whereas "sail:lab" is intended to map the reality by a physical model. Especially the last point presents a challenge on the screen-design. Both an intuitive handling and an easy approach to the physical parameters are required.
The graphical user interface (GUI) is composed of three different frames. On the left we find the input frame, where the physical input parameters (wind and current data, pressure, sailor's weight etc) have to be defined. The output frame on the right provides the current values of the simulation (velocity, course etc). The fundamental difference of input and output panel is emphasized by the use of different design. While simple sliders are chosen at the first board, the output indicators are designed to make associations with instruments known in sailing practise.
The most important component of the GUI is the graphical illustration of the boat with a control unit for sail-, rudder- and fin position and also the position of the sailor on the boat. The diversification of the setting via the control unit is instantaneously executed and presented in the GUI. So, "sail:lab" enables intuitive virtual sailing, especially for sailing experienced users.
As an option also, the various wind-directions, the forces acting on the boat and the sail can be visualized. In particular this is important when sailing is researched from a physical point of view. Also non-sailing-experienced users may take advantage from this additional option.

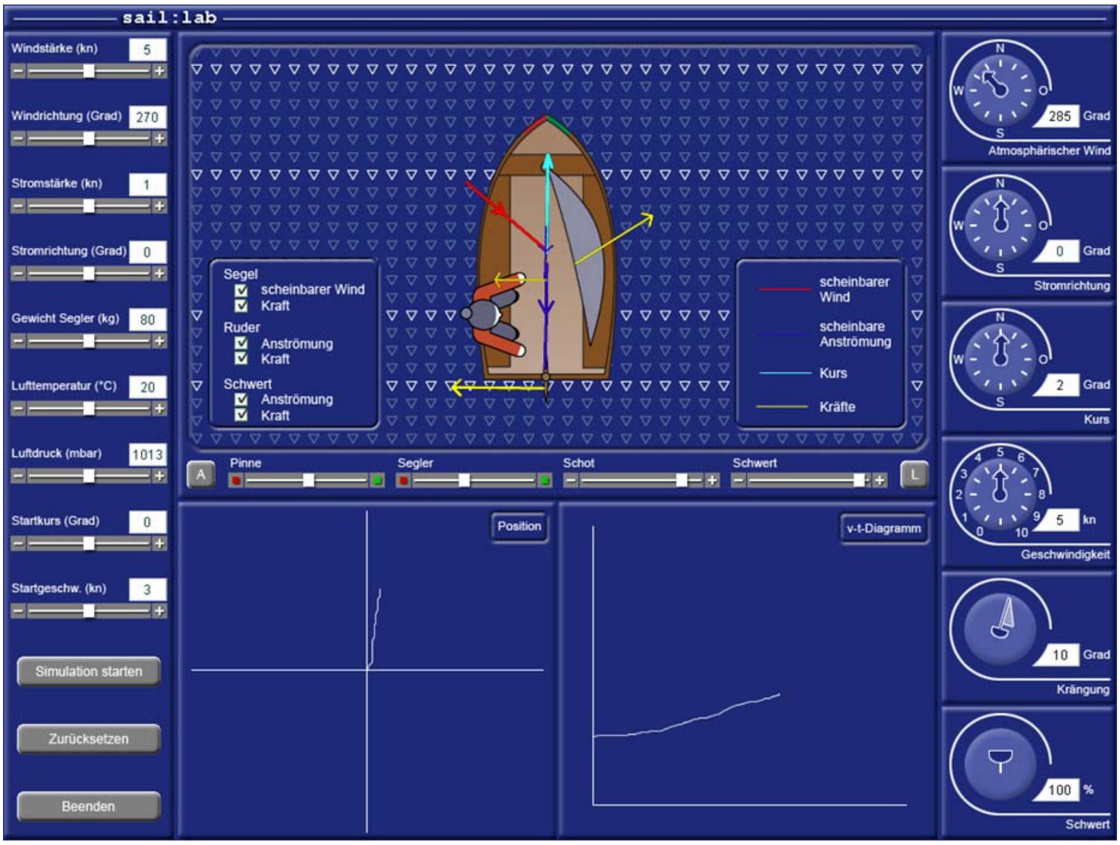

Figure 17: The “sail:lab”-Interface.

Use

The distinctiveness of the application is the integration into the education of different departments of the university. In mathematics, the simulation has an example character in the field of differential equations. This suggests a deployment in lectures for modelling of the department of mathematics. In sport studies “sail:lab” supports the reflection and analyses of the practical moving-experience.

Hence we see “sail:lab” as a learning object, which can be interpreted context-sensitive: In sport studies “sail:lab” serves the purpose of reflection and inspection of the transfer from theory to practical experience in sailing from a learners point of view. In the learning context of mathematics, “sail:lab” presents an ideal type example of mathematical modelling of technical process, simulation and analysis. Furthermore a simulation like “sail:lab” exemplifies the mathematical matters and motivates an indepth contention, which is especially an important benefit for teaching export in natural and engineering sciences.

Beyond the perspective of access, the context sensitivity refers to the teaching-learning-situation, as well: “sail:lab” could be used in a blended-learning-scenario, which enables the learners to find solutions to problem domains, that were raised in lessons. This can be achieved by manipulating and working on the learning object (cf. Hebbel-Seeger, 2005). Likewise sail:lab offers the deployment in lessons, by enabling a teacher to visualise sailing theory, as well as an example for the use of differential equations.

References

Dormand, J. R. & Prince, P. J. (1980). A family of embedded Runge-Kutta formula. Journal of Computational and Applied Mathematics, 6, 19-26.

Hebbel-Seeger, A. (2003). „e-törn“ - interaktive Simulation und Lernhilfe zur Sportart Segeln. dvs-Informationen, 18, 35-36.

Hebbel-Seeger, A. (2005). Towards the integration of face-to-face and distance teaching in sport science by use of a learning platform. Interactive Educational Multimedia, 11, 227-236.

Kibele, A. (2005). Multimodales Lernen in multimedialen Lernumgebungen: Theoriebereich Biomechanik. In J. Wiemeyer (Ed.), Education, Research and New Media, Chances an Challanges for Science (p. 104 – 109). Hamburg: Czwalina.

Papacostas, S. N. & Papageorgiou, G. (1996). A Family of Fifth-Order Runge-Kutta Pairs. Mathematics of Computation 65, 215, 1165-1181.

Perl, J., Lames, M. & Glitsch, U. (Eds.) (2002). Modellbildung in der Sportwissenschaft. Schorndorf: Hofmann.

Attitudes and Behaviors of University PE Students Towards the Use of Computers

E. Bebetsos, O. Kouli, P. Antoniou

Democritus University of Thrace, Komotini, Hellas

Abstract

The aim of this study was to discover the attitudes and behaviors of Greek Physical Education students towards the subject of computers, and the changes that might have occurred in these attitudes and behaviors, as influenced by general information provided in their classrooms. The sample consisted of 244 freshmen students, 119 males and 125 females. They completed a planned behavior questionnaire in the beginning and again in the end of a semester period. The results indicated gender differences and contribution of the variables "knowledge" and "information". Overall, the results supported the use of the instrument as an appropriate tool in order to investigate attitudes and behaviors towards the use of computers.

KEY WORDS: PLANNED BEHAVIOR, ATTITUDES, BEHAVIORS, KNOWLEDGE, INFORMATION

Introduction

According to the theory of reasoned action, a subject's behavior is preceded by that subject's intention. The probability of performing a specific behavior is referred to as 'behavioral intention'. The stronger the intention of a subject, the greater the likelihood that the subject will behave according to his or her intention (Ajzen & Fishbein, 1980). Intention is determined by a combination of two factors: (i) attitude towards the behavior (that is, a positive or negative predisposition towards a specific behavior); and (ii) subjective norms (Ajzen & Fishbein, 1972). These subjective norms are of two kinds: (i) behavioral beliefs (which affect attitude towards the behavior); and (ii) normative beliefs (which reflect social factors). Each behavioral belief reflects whether important others would approve or disapprove of the behavior (Tesser & Shaffer, 1990). The reasoned action model is effective in examining behaviors over which individuals have high control (Theodorakis, 1994).

According to planned behavior theory (Ajzen, 1987; Ajzen, 1988), the execution of a behavior does not relate only to the person's intention. Although a behavior can be totally under a subject's control, in most cases various obstacles are present which impinge on the person's decision to execute a particular behavior. Such obstacles can be internal factors (such as agility, knowledge, and planning), or external factors (such as time, opportunity, cooperation with others, and so on) (Ajzen & Madden, 1986).

Two other variables have been added to the main model of planned behavior theory in order to predict exercise behavior (Theodorakis, 1994). These variables are role identity (a particular social object that represents a dimension of the self) and attitude strength (a variable that expresses how positive, strong, and important are the attitudes towards a given behavior). The first of these, role identity, serves as a link between the individual self and society (Callero, 1985). It is based on Burke's (1980) identity theory in which an individual's self-concept is organised into a hierarchy of role identities that correspond to one's position in the social structure. These might include being a parent, a spouse, or an employee (Charng, Piliavin & Callero, 1988).

Information has often been mentioned as an important factor in understanding how behavior is consistent with attitude (Ajzen & Madden, 1986; Krosnick et al., 1993; Theodorakis, 1994; Bebetsos, Antoniou, Kouli, & Trikas, 2004). Limited information and knowledge about the behavior can represent a serious obstacle, preventing individuals from carrying out the behavior in question (Theodorakis, 1994). Therefore, absence of this factor can reduce the accuracy of any assessment of the behavior. Information is a construct that has not received much attention in recent research based on planned behavior theory. Although it is frequently reported as being an important factor in the literature on attitude, few studies provide a clear definition of it—although Krosnick et al. (1993) did define information (or, rather, *interest in* relevant information, to use their terminology) as being 'the extent to which an individual is motivated to gather information about an attitude object' (p. 1133).

Investigators have already used the theory of planned behaviour to predict behaviours in a variety of exercise settings: intention to participate in sports and physical activities (Godin & Shephard, 1986), intention of pregnant women to exercise after giving birth (Godin, Vezina & Leclerc, 1989), participation in sports and physical activities (Theodorakis, Doganis, Bagiatis & Goudas, 1991; Theodorakis, 1994), and jogging (Riddle, 1980). Also, studies utilized the theory to understand intention to participate in aerobics (Gatch & Kendzierski, 1990), in sports and physical activity (Dzewaltowski, Noble & Shaw, 1990; Bebetsos, Antoniou, Kouli, & Trikas, 2004), in exercise (Hausenblas, Carron & Mack, 1997; Symons, Downs & Hausenblas, 2001; Hagger, et al., 2002) and in team training of young swimmers (Theodorakis, 1992). Finally, validity of the theory was investigated in different healthy and unhealthy behaviours such as dieting (Povey, Conner, Sparks, James & Shepherd, 2000), alcohol use (Rise & Wilhelmson, 1998), safer sex (Sheeran, Abraham, Orbell, 1999; Sutton, McVey & Glanz, 1999), health screening (Conner & Sparks, 1996; Godin & Kok, 1996; Armitage & Conner, 2000; Sheeran, Conner, Norman, 2001) smoking, exercising, and eating-habit domains (Norman & Smith, 1995; Sheeran & Orbell, 2000; Bebetsos, Chroni, & Theodorakis, 2002; Bebetsos, Papaioannou, & Theodorakis, 2003) and moral functioning (Bebetsos & Konstantoulas, 2006).

In the present investigation, planned behavior theory was used to predict the behaviors and attitudes of Greek Physical Education university students towards computers. In addition, we studied any changes that might have occurred in these attitudes and behaviors after a four-month period, as influenced by general information that was provided in the classrooms. Gender differences were also checked.

Methods

Subjects and procedure

The sample consisted of 244 freshmen students, 119 males and 125 females between the ages of 17-27 (M±18.5).

All subjects completed a planned behavior theory questionnaire (Ajzen & Madden, 1986).. The greek version of the questionnaire (Theodorakis, 1994) was used in two different periods—a 'pre-test' took place at the beginning of the fall semester (November) and a 'post-test' took place at the beginning of the spring semester (March).

The aim of this study was to examine the attitudes and intentions towards the subject of computers, gender differences, and to note any changes that might have occurred after the end of a four-month period (semester course).

More specifically, the components of the questionnaire were:

Intention was estimated by the mean-score [mean score was produced from the summary of variables data divided by the number of variables (i.e. 21/3=7,0). This compute transformed the data type from ordinal type to scale] of the responses to three different questions: "I intend/I will try/ I am determined to use computers regularly for the next 2 months" Responses to the first question (I intend…) were rated on a 7-point scale from 1=very unlikely to 7=very likely. A 7-point scale with endpoints labelled 1=definitely no to 7=definitely yes, was used for the other two questions.

Attitudes were estimated by the mean score of responses to the question "For me to use computers regularly for the next 2 months is…". Responses were rated on 7-point scale, on six bipolar adjectives (7=good – 1=bad, 1=foolish – 7=smart, 7=healthy – 1=unhealthy, 7=useful – 1=unuseful, 7=nice – 1=ugly, 7=pleasant – 1=unpleasant).

Subjective Norms were estimated by the mean score of responses to four questions "If I to use computers regularly for the next 2 months, individuals who are important to me…"; "Generally, I enjoy doing what some important individuals want me to do"; "Some individuals who are important in my life, believe that I must use computers regularly for the next 2 months"; "Generally, I like doing what some important individuals want me to do". Responses were rated on 7-point scales. For questions 1, 2 and 4 responses were rated on 1 = will strongly disagree, to 7 = will strongly agree and for question 3 responses were 1 = very impossible, to 7 = very possible.

Perceived behavioural control for the specific behavior was estimated by the mean-score on three questions. Examples of questions were: "If I wanted to, I could use computers regularly for the next 2 months", "For me to use computers regularly for the next 2 months is…", "How much control do you exert over using computers regularly for the next 2 months?" A 7-point scale was used, ranging from 1=very unlikely to 7=very likely, for the first question, from 1=difficult to 7=easy for the second and 1=no control to 7=complete control for the third, respectively.

Role Identity was measured by four questions: "I consider myself to be able to use computers regularly for the next 2 months"; "I consider myself a person that will use computers regularly for the next 2 months"; "Its in my character (temperament) to use computers regularly for the next 2 months"; "Generally, I am the type who is going to be using computers regularly for the next 2 months". Responses were rated on 7-point scales from 1=strongly disagree to 7=strongly agree. This scale was adapted from Theodorakis (1994).

Attitude Strength was measured using eight questions (Theodorakis, 1994). The items were: "How certain are you that you are using computers regularly for the next 2 months?"; "Is it right for you to use computers regularly for the next 2 months?"; "I feel very sure that I will use computers regularly for the next 2 months"; "Is it important for you personally, to use computers regularly for the next 2 months?"; "How interested are you in using computers regularly for the next 2 months?"; "For me to use computers regularly for the next 2 months …"; "With the knowledge I have, I think I will use computers regularly for the next 2 months"; "Do you find it interesting to use computers regularly for the next 2 months?". Responses were rated on 7-point scales, for the first item from 1=very uncertain to 7=very certain, for the second and sixth items from 1=not at all to 7=very much so, for the third and seventh items from 1=strongly disagree to 7=strongly agree, for the fourth item from 1=not important at all to 7=very important and for the fifth and eighth items from 1=not at all to 7=very much.

Knowledge about the specific subject was measured by the mean score of responses to four questions: "Some of us are very well informed about using computers regularly, while other individuals aren't. How well informed about using computers regularly do you believe that you are?"; "If someone told you to write anything you know about using computers regularly, how much could you write?"; "In comparison to other students, I believe that I am very well informed on the issue of using computers regularly", "How much do you think that you know on the issue of using computers regularly?". The answers were rated on 7-point scales. For the first question from 1=not informed at all to 7=very well informed, for the second question from 1=very little to 7=a lot, for the third from 1=I strongly disagree to 7=I strongly agree and for the last question from 1=no knowledge at all to 7=a lot of knowledge. This scale was adapted from Theodorakis (1994).

Information was measured by four questions: "Some individuals told me that they pay attention to different information about using computers regularly. How much attention do you pay to different information about using computers regularly?"; "How often do you pay attention to different printed material with information about using computers regularly?"; "I am very interested in any information regarding using computers regularly"; "How often do you pay attention to information regarding using computers regularly?". Responses were given on 7-point scales, for the first and fourth questions from 1=I never pay attention to 7=I very much pay attention, for the second from 1=never to 7=very often, for the third from 1=I strongly disagree to 7=I strongly agree and for the fourth from 1=I never pay attention to 7=I pay a lot of attention. This scale was adapted from Theodorakis (1994).
The same questionnaire was completed in the post-test phase.

Descriptive statistics: Inspection of Table 1 indicates that all scales of the questionnaire demonstrated acceptable internal consistency—that is, for all of them, Cronbach's alpha was higher than 0.66.

Results

Gender Differences

Univariate analyses were conducted in order to find any gender differences. The analyses revealed statistical significant gender differences in almost all variables.

(a) For the variable of *attitudes:* $F(1,446)=10{,}70$, $p<.01$. Men had higher scores (M=5,65, SD=.67) than women (M=5,43, SD=.77).

(b) For the variable of *intention:* $F(1,456)=12{,}66$, $p<.001$. Men had higher scores (M=5,44, SD=1,12) than women (M=5,03, SD=1,31).

(c) For the variable of *role identity:* $F(1,455)=6{,}50$, $p<.01$. Men had higher scores (M=4,91, SD=1,12) than women (M=4,61, SD=1,12).

(d) For the variable of *attitude strength:* $F(1,452)=9{,}03$, $p<.01$. Men had higher scores (M=5,22, SD=.93) than women (M=4,92, SD=1,01).

(e) For the variable *subjective norms:* $F(1,452)=18{,}90$, $p<.001$. Women had higher scores (M=4,82, SD=1,24) than men (M=4,331, SD=1,24).

No gender differences were found on the variable of *perceived behavioural control*.

Table 1. Internal validity factors and descriptive characteristics of all variables and scale means of the repeated measures analyses

Variables	Mean (±sd)	Number of subjects	Cronbach's alpha
Pre-test			
Attitudes	5.52(±0.7)	6	0.70
Intention	5.33(±1.2)	3	0.73
Subjective norms	4.61 (±1.3)	4	0.70
Role identity	4.73 (±1.2)	4	0.80
Perceived behavioral control	4.96(±1.1)	3	0.68
Attitude strength	5.12 (±1)	8	0.86
Knowledge	2.85(±1.1)	4	0.85
Information	3.64 (±1.3)	4	0.83
Post-test			
Attitudes	5.53(±0.7)	6	0.70
Intention	5.12 (±1.3)	3	0.79
Subjective norms	3.82 (±1.1)	4	0.66
Perceived behavioral control	4.74(±1.2)	3	0.70
Role identity	4.77 (±1.2)	4	0.75
Attitude strength	5 (±1)	8	0.87
Knowledge	3.44(±1.1)	4	0.84
Information	3.99(±1.2)	4	0.83

For the variable of *information* no gender differences were revealed. On the other hand, the analysis indicated statistical significant differences between the two measurements $F(1,457)=8,5$, $p<.01$, were the sample had higher scores on the second measurement (M=3,99, SD=1,24) than the first (M=3,64, SD=1,28). Finally, for the variable of *knowledge* no gender differences were revealed. On the other hand the analysis indicated statistical significant differences between the two measurements $F(1,455)=29,22$, $p<.001$, were the sample had higher scores on the second measurement (M=3,44, SD=1,15) than the first (M=2,85, SD=1,15).

Discussion

The purpose of this study was to investigate if planned behavior theory can predict the behaviors and attitudes of PE University students towards computers. The analyses and their results supported the validity of the planned behavior model for prediction of attitudes and behaviors of the students.

More specifically, the results indicated first, gender differences on the variable of attitudes, intentions, attitude strength, and role identity. Men had stronger attitudes and behaviours toward the use of computers than women. Previous research has shown mixed results. Schumacher and Moharan-Martin (2001) underlined that women generally have less computer experience than men, with result to have negative attitudes towards computers. Also, Ho and Lee (2001) reported in the study that male students have more computer experience than female students, and boys tend to have less computer anxiety, more positive attitudes toward computers and higher computer confidence than girls. In an earlier study, Nash and Moroz (1997) found out that the gender of a person does not have an effect on the persons' attitudes towards computers, rather than his/her actions do have the effect. Finally, in a previous study in a sample of Greek high school students, Antoniou, Patsi, Bebetsos and Ifantidou (2006) found no gender differences.

Additionally, results also indicated gender differences on the variable of subjective norms. Women indicated that were more dependent on the other important people's opinion on the computer issue. Earlier studies supported these result on other subjects such as smoking, exercising and eating habits (Bebetsos, Chroni, & Theodorakis, 2002; Bebetsos, Papaioannou, & Theodorakis, 2003).

Finally, the results revealed the importance of two more variables, knowledge and information. Previous studies have also shown the important role that knowledge and information play on the formation of positive opinion and intentions of the people (Bebetsos, Antoniou, Kouli, & Trikas, 2004). Consistent with other studies (Davidson, Yantis, Norwood, & Montano, 1985; Wilson, Kraft, & Dunn, 1989; Krosnick, et al., 1993, Theodorakis, 1994), results indicated that the amount of information and knowledge available about a specific subject might be a determinant of consistency between attitude and action. The results of the present study indicated that the computer course increased the amount of knowledge and information of the students which might plays an important role for the contribution in the configuration of positive attitudes towards computer use.

Generally, many conclusions were drawn on the subject of the use of computers in education. McMamhn, Garder, Gray and Mulhen (1999) tried to find the barriers to student use of computers in Universities across United Kingdom. Their results showed that students identified lack of training as the most important factor that kept them away from computer use. They believed that the training they received was inadequate. On the other hand, staff members supported the idea of self-help as a very important factor for the students' computer learning process. However in some instances, anxiety and lack of confidence interacted to prevent students from adopting this approach. Students also felt that the support they were getting from the University staff members on using computers was not the appropriate one. Finally, access to computers was also an important factor.

On another study, Usun (2003) investigated undergraduate students' attitudes towards educational uses of the internet. His results suggested that all universities should use the internet for education purposes. Also, computer university courses should encourage students to use computers and internet in order to improve their academic status, knowledge and it also improve their learning capability.

Research has shown the direct relationship between the use of computers and physical activity. Thomas and Stratton (2006) in their study on the importance of use of information communication technology in physical education classes showed that Physical Education teachers had very positive opinion on the integration of information communication technology into their classes and believed that the use of technology as is a valuable tool in promoting effective teaching and learning. Nigg (2003) argued that the use of technology is related to a decline in physical activity. However, he made some very important points on how technology can influence positively physical activity. He pointed out that technology can help on the large of recruitment of populations, can individualize interventions and promote different physical activity interventions on large populations in different ways.

Other research supported the opinion that computer use can enhance physical activity. Ho and Lee (2001) in their research on computer use and its relation to adolescent lifestyle in Hong Kong found some very interesting results. Their sample consisted of 2110 secondary school students. The results indicated that the total amount of time spent on computers was not associated with any social or physical lifestyle. More specifically, their data showed that computers users have more active lifestyle including more exercise and recreational activities. Additionally, they found out that boys, heavier computer users exercise more than boys who just use computers to play games. The latest study of Koezuka, Koo, Allison, Adlaf, Dwyer, Faulkner, and Goodman (2006) supported the above results. Their sample, 7982 Canadian youth, indicated that computer use is a protective factor against inactivity among males and was not significantly related to physical inactivity among females. More specifically, males using computers for less than six hours/week, were about 40% less likely to be inactive compared to nonusers. Their results suggest that the time spent on computers may not necessarily replace time spent on physical activity.

Overall, the study supported the use of the planned behaviour instrument on examining the attitudes and intentions of people towards another subject such as the use of the computers. Possible limitations of the present investigation should be mentioned. All participants were freshmen university students who might be cognizant of the benefits of the use of the computers. Future research should continue investigating similar and other aspects that effect peoples' attitudes and intentions towards computer use.

References

Ajzen, I. (1987) Attitudes, traits and actions: Dispositional prediction of behavior in personality and social psychology. In L. Berkowitz (ed.), *Advances in experimental social psychology*. . New York: Academic Press. Pp. 1-63.

Ajzen, I. (1988) *Attitudes, personality, and behavior*. Bristol Eng.: Open Univer. Press.

Ajzen, I., & Fishbein, M. (1972) Attitudes and normative beliefs as factors influencing behavioral intentions. *Journal of Personality and Social Psychology*, 21, 1–9.

Ajzen, I., & Fishbein, M. (1980) *Understanding attitudes and predicting social behavior*. Englewood Cliffs, NJ: Prentice-Hall.

Ajzen, I., & Madden, T. J. (1986) Predictions of goal-directed behavior: Attitudes, intentions and perceived behavioral control. *Journal of Experimental Social Psychology,* 22, 453–457.

Antoniou, P., Patsi, H., Bebetsos, E., & Ifantidou, G. (2006) Validity of scale and evaluation of students' attitudes toward computers. Compare with students' attitudes toward physical education and physical activity. *Inquiries in Sport & Physical Education, 4 (1),* 114-124.

Armitage, C. J., & Conner, M. (2000) Social cognition models and health: a structured review. *Psychology and Health*, 15, 173-189.

Bebetsos, E., Chroni, S., & Theodorakis, Y. (2002) Physically active students' intentions and self-efficacy towards healthy eating. *Psychological Reports*, 92, 485-495.

Bebetsos, E., Papaioannou, A., & Theodorakis, G. (2003) University students' attitudes and behaviours towards smoking and exercise. *European Journal of Physical Education,* 8, 29-51.

Bebetsos, E., Antoniou, P., Kouli, O., Trikas, G. (2004) Knowledge and information in prediction of intention to play badminton. *Perceptual and Motor Skills, 98,* 1210-1218.

Bebetsos, E., & Konstantoulas, D. (2006). Contact sports, moral functioning and planned behaviour theory. *Perceptual and Motor Skills, 103,* 131-144.

Burke, P. J. (1980) Measurement requirements from an interactionist perspective. *Social Psychology Quarterly*, 43, 18–29.

Callero, P. L. (1985) Role-identity salience. *Social Psychology Quarterly,* 48, 203–215.

Charng, H. W., Piliavin, J. A., & Callero, P. L. (1988) Role identity and reasoned action in the prediction of repeated behavior. *Social Psychology Quarterly,* 51, 303–317.

Conner, M., & Sparks, P. (1996) The theory of planned behavior. In M. Conner, & P. Norman (Eds.), *Predicting health behaviour: research and practice with social cognition models.* Buckingham, England: Open Univer. Press (pp. 121-162).

Davidson, A. R., Yantis, S., Norwood, M., & Montano, D. E. (1985) Amount of information about the attitude object and attitude-behavior consistency. *Journal of Personality and Social Psychology*, 49, 1184-1198.

Dzewaltowski, D. A., Noble, J. M., & Shaw, J. M. (1990) Physical activity participation: social cognitive theory versus the theories of reasoned action and planned behavior. *Journal of Sport and Exercise Psychology*, 12, 388-405.

Gatch, L. C., & Kendzierski, D. (1990) Predicting exercise intentions: the theory of planned behavior. *Research Quarterly for Exercise and Sport*, 61, 100-102.

Godin, G., & Shephard, R. J. (1986) Psychosocial factors influencing intentions to exercise of young students from grades 7 to 9. *Research Quarterly for Exercise and Sport*, 57, 44-52.

Godin, G., Vezina, L., & Leclerc, O. (1989) Factors influencing intentions of pregnant women to exercise after giving birth. *Public Health Reports*, 104, 188-196.

Godin, G., & Kok, G. (1996) The theory of planned behaviour: A review of its applications to health-related behaviours. *American Journal of Health Promotion*, 11, 87-97.

Hagger, M. S., Chatzisarantis, N. L. D., & Biddle, S. J. H. (2002) A meta-analytic review of the theories of reasoned action and planned behavior in physical activity: predictive validity and the contribution off additional variables. *Journal of Sport and Exercise Psychology*, 24, 1-12.

Hausenblas, H. A., Carron, A. V., & Mack, D. E., (1997) Application of the theories of reasoned action and planned behaviour to exercise behaviour: a meta-analysis. *Journal of Sport and Exercise Psychology*, 19, 36-51.

Ho, S. M. Y., & Lee, T. M. C. (2001) Computer usage and its relationship with adolescent lifestyle in Hong Kong. *Journal of Adolescent Health*, *29*, 258-266.

Koezuka, N. M., Koo, M., Allison, K. R., Adlaf, E. M., Dwyer, J. J. M., Faulkner, G., & Goodman, J. (2006) The relationship between sedentary activities and physical inactivity among adolescents: Results from the Canadian Community Health Survey. *Journal of Adolescent Health*, *39*, 515-522.

Krosnick, J. A., Boninger, D. S., Chuang, Y. C., Berent, M. K., & Carnot, C. G. (1993) Attitude strength: one construct or many related constructs?. *Journal of Personality and Social Psychology*, 65, 1132–1151.

McMahon, J., Garder, J., Gray, C., & Mulhen, G. (1999) Barriers to student computer usage: staff and student perceptions. *Journal of Computer Assisted Learning*, *15*, 302-311.

Nash, J., & Moroz, P. (1997) Computer attitudes among professional educators: the Role of gender and experience. Annual Meeting of the Southwest Educational Research Association, 23-27.

Nigg, C. R. (2003) Technology's influence on physical activity and exercise science: The present and the future. *Psychology of Sport and Exercise*, *4*, 57-65.

Povey, R., Conner, M., Sparks, P., James, R., & Shepherd, R. (2000) Application of the theory of planned behaviour to two dietary behaviours: roles of perceived control and self- efficacy. *British Journal of Social Psychology*, 5, 121-139.

Riddle, K. P. (1980) Attitudes, beliefs, behavioral intentions, and behaviors of women and men toward regular jogging. *Research Quarterly for Exercise and Sport*, 51, 663-674.

Rise, J., & Wilhelmson, B. U. (1998) Prediction of adolescents' intention not to drink alcohol: Theory of planned behaviour. *American Journal of Health Behaviour*, 22, 206-217.

Schumacher, P., & Moharan-Martin, T. (2001) Gender, Internet and computer experiences. *Computers in Human Behavior*, *17*, 95-110.

Sheeran, P., Abraham, C., & Orbell, S. (1999) Psychosocial correlates of heterosexual condom use: A meta-analysis. *Psychological Bulletin,* 125, 90-132.

Sheeran, P., Conner, M., & Norman, P., (2001) Can the theory of planned behaviour explain patterns of health behaviour change? *Health Psychology,* 20, 12-19.

Symons, S., Downs, D., & Hausenblas, H. A. (2001) Applying the theories of reasoned action and planned behaviour to exercise: a meta-analytic update. Paper presented at the Association for the Advancement of applied sport psychology, Orlando, Florida.

Sutton, S., McVey, D., & Glanz, A. (1999) A comparative test of the theory of reasoned action and the theory of planned behaviour in the prediction of condom use in a national sample of English young people. *Health Psychology,* 18, 72-81.

Tesser, A., & Shaffer, D. R. (1990) Attitudes and attitude change. *Annual Review Psychology,* 41, 479–523.

Theodorakis, Y., Doganis, G., Bagiatis, K. & Goudas, M. (1991) Preliminary study of the ability of reasoned action model in predicting exercise behavior of young children. *Perceptual and Motor Skills*, 72, 51-58.

Theodorakis, Y. (1992) Prediction of athletic participation: a test of planned behavior theory. *Perceptual and Motor Skills,* 74, 371-379.

Theodorakis, Y. (1994) Planned behavior, attitude strength, self-identity, and the prediction of exercise behavior. *The Sport Psychologist,* 8, 149–165.

Thomas, A., & Stratton, G. (2006) What we are really doing with ICT in physical education: a national audit of equipment, use teacher attitudes, support, and training. *British Journal of Educational Technology, 37 (4),* 617-632.

Usun, S. (2003) Undergraduate students attitudes towards use of internet. *Interactive Educational Multimedia, 7,* 46-62.